Tran-SET

Transportation Consortium of South-Central States

Solving Emerging Transportation Resiliency, Sustainability, and Economic Challenges through the Use of Innovative Materials and Construction Methods: From Research to Implementation

Holistic Network-level Assessment of Pavement Flood Damages

Project No. [19PLSU13]

Lead University: [Louisiana State University]

Collaborative Universities: [Texas A&M University]

Final Report

December 2020

Disclaimer

The contents of this report reflect the views of the authors, who are responsible for the facts and the accuracy of the information presented herein. This document is disseminated in the interest of information exchange. The report is funded, partially or entirely, by a grant from the U.S. Department of Transportation's University Transportation Centers Program. However, the U.S. Government assumes no liability for the contents or use thereof.

Acknowledgements

The research team would like to thank you the Project Review Committee including Christophe Fillastre, Dr. Silvana V Croope, and Michael A. Frabizzio for their insightful suggestions and feedback. In addition, we would like to express our appreciation to Angela H. Murrell and Christophe Fillastre to provide Louisiana PMS data.

TECHNICAL DOCUMENTATION PAGE

1. Project No.	2. Government Accession No.	3. Recipient's Catalog No.
19PLSU13		

4. Title and Subtitle	5. Report Date
	December. 2020
Holistic Network-level Assessment of Pavement Flood Damages	**6. Performing Organization Code**
7. Author(s) Dr. Yong-Cheol Lee Dr. Kunhee Choi Moeid Shariatfar	**8. Performing Organization Report No.**
9. Performing Organization Name and Address Transportation Consortium of South-Central States (Tran-SET)	**10. Work Unit No. (TRAIS)**
University Transportation Center for Region 6 3319 Patrick F. Taylor Hall, Louisiana State University, Baton Rouge, LA 70803	**11. Contract or Grant No.** 69A3551747106
12. Sponsoring Agency Name and Address United States of America Department of Transportation	**13. Type of Report and Period Covered** Final Research Report August. 2019 – December. 2020
Research and Innovative Technology Administration	**14. Sponsoring Agency Code**

15. Supplementary Notes

Report uploaded and accessible at Tran-SET's website (http://transet.lsu.edu/).

16. Abstract

After recent catastrophic flood disasters in Louisiana in 2016 and Texas in 2017, roadways in Region 6 areas suffer not only from the flood-inundation, but also from the long-term recovery processes that incur enormous maintenance costs. To assess the impacts of flooding disasters on roadways, various studies have investigated sampled roadway damages with pavement engineering techniques such as a direct damage analysis using cores/bores. However, current methods are time-consuming and labor-intensive. In addition, even though existing methods provide a detailed damage analysis of pavement in a particular location for a particular time period, there is still a large practical knowledge gap in understanding network-level roadway functional/structural damages before-and-after historic flooding as well as assessing flooding impacts on roadways over time. Thus, a holistic perspective and a long-term investigation on roadway damages caused by floods have been rarely addressed, which has resulted in the absence of accurate maintenance cost prediction. The primary objective of this project is to develop a holistic roadway damage assessment method using the flood models and the pavement condition data accumulated over the years. This project also aims to provide a means for Louisiana and Texas (ultimately to all Region 6's States) to intuitively identify roadway damage patterns at the network level caused by flooding over time as well as predict roadway maintenance tasks. To accomplish the proposed goal, this project examines roadways of parishes and counties in Louisiana and Texas affected by previous flood disasters by using pavement assessment data obtained from the Pavement Management System (PMS) in the Louisiana Department of Transportation and Development (LaDOTD), and the Pavement condition data of the City of Houston. This project is expected to provide a network-level roadway damage assessment and play a pivotal role in reducing the cost of a direct damage analysis such as coring/boring.

17. Key Words	18. Distribution Statement
Pavement performance, PMS, flooding damage, prediction model	No restrictions. This document is available through the National Technical Information Service, Springfield, VA 22161.

19. Security Classif. (of this report)	20. Security Classif. (of this page)	21. No. of Pages	22. Price
Unclassified	Unclassified	[50]	

Form DOT F 1700.7 (8-72) **Reproduction of completed page authorized.**

SI* (MODERN METRIC) CONVERSION FACTORS

APPROXIMATE CONVERSIONS TO SI UNITS

Symbol	When You Know	Multiply By	To Find	Symbol
		LENGTH		
in	inches	25.4	millimeters	mm
ft	feet	0.305	meters	m
yd	yards	0.914	meters	m
mi	miles	1.61	kilometers	km
		AREA		
in^2	square inches	645.2	square millimeters	mm^2
ft^2	square feet	0.093	square meters	m^2
yd^2	square yard	0.836	square meters	m^2
ac	acres	0.405	hectares	ha
mi^2	square miles	2.59	square kilometers	km^2
		VOLUME		
fl oz	fluid ounces	29.57	milliliters	mL
gal	gallons	3.785	liters	L
ft^3	cubic feet	0.028	cubic meters	m^3
yd^3	cubic yards	0.765	cubic meters	m^3
		NOTE: volumes greater than 1000 L shall be shown in m^3		
		MASS		
oz	ounces	28.35	grams	g
lb	pounds	0.454	kilograms	kg
T	short tons (2000 lb)	0.907	megagrams (or "metric ton")	Mg (or "t")
		TEMPERATURE (exact degrees)		
°F	Fahrenheit	5 (F-32)/9 or (F-32)/1.8	Celsius	°C
		ILLUMINATION		
fc	foot-candles	10.76	lux	lx
fl	foot-Lamberts	3.426	$candela/m^2$	cd/m^2
		FORCE and PRESSURE or STRESS		
lbf	poundforce	4.45	newtons	N
lbf/in^2	poundforce per square inch	6.89	kilopascals	kPa

APPROXIMATE CONVERSIONS FROM SI UNITS

Symbol	When You Know	Multiply By	To Find	Symbol
		LENGTH		
mm	millimeters	0.039	inches	in
m	meters	3.28	feet	ft
m	meters	1.09	yards	yd
km	kilometers	0.621	miles	mi
		AREA		
mm^2	square millimeters	0.0016	square inches	in^2
m	square meters	10.764	square feet	ft^2
m	square meters	1.195	square yards	yd^2
ha	hectares	2.47	acres	ac
km	square kilometers	0.386	square miles	mi^2
		VOLUME		
mL	milliliters	0.034	fluid ounces	fl oz
L	liters	0.264	gallons	gal
m	cubic meters	35.314	cubic feet	ft^3
m	cubic meters	1.307	cubic yards	yd^3
		MASS		
g	grams	0.035	ounces	oz
kg	kilograms	2.202	pounds	lb
Mg (or "t")	megagrams (or "metric ton")	1.103	short tons (2000 lb)	T
		TEMPERATURE (exact degrees)		
C	Celsius	1.8C+32	Fahrenheit	°F
		ILLUMINATION		
lx	lux	0.0929	foot-candles	fc
cd/m^2	$candela/m^2$	0.2919	foot-Lamberts	fl
		FORCE and PRESSURE or STRESS		
N	newtons	0.225	poundforce	lbf
kPa	kilopascals	0.145	poundforce per square inch	lbf/in^2

TABLE OF CONTENTS

LIST OF FIGURES

LIST OF TABLES

ACRONYMS, ABBREVIATIONS, AND SYMBOLS

ADT	Average Daily Traffic
AADT	Annual Average Daily Traffic
ASP	Asphalt Pavement
COM	Composite Pavement
DOT	Department of Transportation
DOTD	Department of Transportation and Development
EICM	Enhanced Integrated Climate Model
EP	Extreme Precipitation
FEMA	Federal Emergency Management Agency
FWD	Falling Weight Deflectometer
GPR	Ground Penetrating Radar
HCD	Historical Climate Data
IRI	International Roughness Index
JCP	Jointed Concrete Pavement
JPCP	Jointed Plain Concrete Pavement
LADOTD	Louisiana Department of Transportation and Development
LTRC	Louisiana Transportation Research Center
MEPDG	Mechanistic-Empirical Pavement Design Guide
Mr	Modulus of Resilience
PMS	Pavement Management System
PMIS	Pavement Management Information System
Pr	Probability of Flooding
RD	Road Deterioration
SVM	Support Vector Machine
TMR-QLD	Transport and Main Roads Authority, Queensland Database
TPM	Transition Probability Matrix
USGS	United States Geological Survey
XGB	XG Boost Classifier

EXECUTIVE SUMMARY

After recent catastrophic disasters, roadways in Region 6 areas suffer not only from the flood-inundation, but also from the long-term recovery processes that incur enormous maintenance costs. Two recent severe flooding events in Texas in August 2017 and Louisiana in August 2016 clearly show how catastrophic events cause direct damages such as sweeping away roadways systems as well as indirect damage such as deteriorating pavement's long-term performance. To assess the impacts of flooding disasters on roadways, various studies have investigated sampled roadway damages with pavement engineering techniques such as a direct damage analysis using cores/bores. However, current methods are time-consuming and labor-intensive. For example, Pielke et al. stated that rebuilding projects in the area affected by Hurricane Katrina in 2005 (State of Louisiana and Mississippi) required $81 billion for completion (Pielke et al. 2008). In addition, this process can take up to five years (FEMA 2005) or even more, up to 10 years (Goodyear 2013), depending on the severity of a disaster and the size of a damaged area. For example, one study (Rowley 2008) claimed that the recovery process of the Hurricane Katrina needed a 10-year period. One previous paper (Chang and Nojima 2001) also stated that the highway reconstruction process after the Hyogoken-Nanbu Earthquake occurred in the Kobe region in Japan took 20 months.

In addition, even though existing methods provide a detailed damage analysis of pavement in a particular location for a particular time period, there is still a large practical knowledge gap in understanding network-level roadway functional/structural damages before-and-after historic flooding as well as assessing flooding impacts on roadways over time. Since each roadway system encompasses several miles of interconnected networks between cities and States in Region 6, a holistic assessment of roadway damages after flooding events not only provides regional roadway damage patterns but also facilitates an integrated roadway recovery and maintenance plan. In addition, one of critical challenges in a post-disaster recovery process for decision makers is a lack of a systematical evaluation process of possible recovery plans that can promptly restore normal livelihood (Karlaftis et al. 2007). Unfortunately, a lack of holistic perspective and a long-term investigation on roadway damages caused by floods has resulted in the absence of accurate maintenance cost prediction.

The primary objective of this project is to develop a holistic roadway damage assessment method using the flood models and the pavement condition data accumulated over the years. This project also aims to provide a means for Louisiana and Texas (ultimately to all Region 6's States) to intuitively identify roadway damage patterns at the network level caused by flooding over time as well as predict roadway maintenance tasks. To accomplish the proposed goal, this project examines roadways in Louisiana and Texas affected by previous flood disasters by using pavement assessment data obtained from the Pavement Management System (PMS) in the Louisiana Department of Transportation and Development (LaDOTD) and the pavement condition data of the City of Houston. Pavement Management Systems in each state DOT and city provide a set of tools that helps consistent pavement condition assessment and road network administration to distribute the data to each county or perish so they can determine the best maintenance and

rehabilitation priorities and strategies (Ferreira et al. 2011). This study analyzed the impact of flood events on roadway pavement and developed a damage pattern analysis method to predict affected pavements in short-term and long-term pavement performance. In particular, this study investigated the impacts of the Louisiana's 2016 flood event on pavement structure by using two different flood maps. The first one is based on the Louisiana 2016 flood maps, and the second flood data source is the FEMA high-risk flood map. For analyzing the impact of flood events on pavement conditions, roadways were separated and categorized based on their locations inside or outside of the flood regions. The results of the analysis conducted based on 2016 flood data showed that the flood event slightly affects the IRI as the IRI score increased after the event and the pavement performance index decreased. In addition, the two prediction models were developed using SVM (Support Vector Machine) and XGB (XG Boost) classifiers, to predict pavement performance in 2017 based on the aforementioned data (PMS, ADT, etc.) for the 2013-2015 period. The model developed based on the estimated 2016 flood data showed 76.2% accuracy, and the model with the FEMA flood data showed 69.8% accuracy. It can be concluded that the estimated 2016 flood data were more accurate compared to FEMA high-risk flood zones. Another prediction model was created using FEMA flood data to predict the pavement performance in 2019 using the data collected from 2013 to 2017. The model's accuracy reached to near 80%.

1. INTRODUCTION

In August 2016, a flood disaster occurred in Louisiana which according to Red Cross was the worst US disaster since hurricane Sandy (Yan and Flores 2016). The incident severely damaged Louisiana's infrastructure systems and caused several road closures due to inundated roadways. Figure 1 is a flood map retrieved from the USGS (United States Geological Survey) Flood Event Viewer that shows the areas affected by the 2016 Louisiana flooding. Roadways can be easily inundated by a flooding and many roadway sections are exposed to flood risk. In August 2017, Hurricane Harvey caused severe damages to infrastructure including roadways in Texas. Several roadways are frequently inundated with floodwater or the stork of debris, providing critical problems in providing the path for evacuation, assistance, and others (Chen and Zhang 2014).

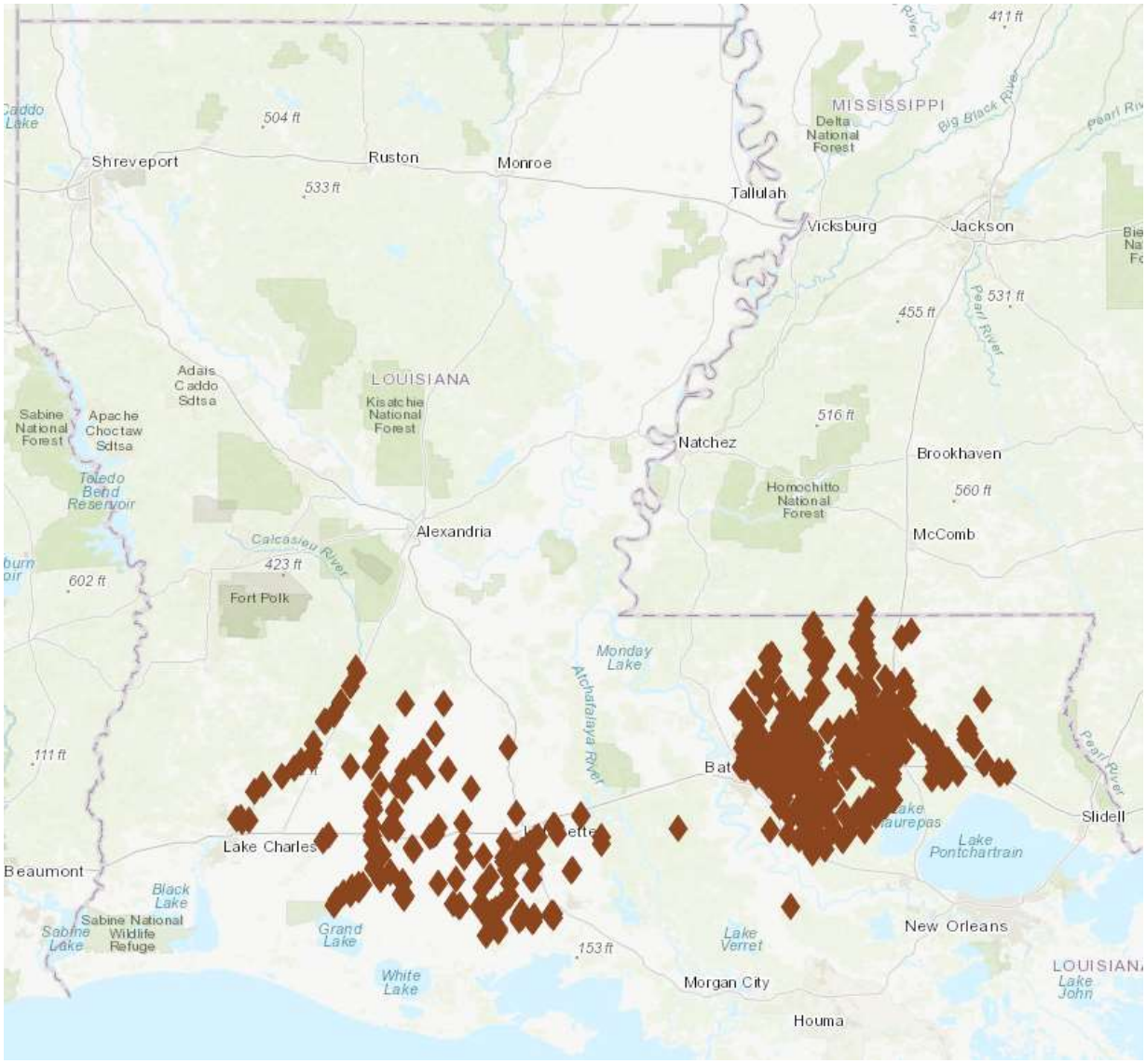

Figure 1: Flooded areas in 2016 Louisiana flood (USGS 2010)

Proper evaluation of flooded pavements and their performance is critical for DOT (Department of Transportation) practitioners to make risk-informed decisions for pavement construction, rehabilitation, and maintenance. These decisions significantly affect system management cost, safety risk, and pavement performance. Most of flood damages on roadway pavement are not visible after the floodwater recedes (Mallick et al. 2017), and thus, a comprehensive investigation is required to estimate the impact of flood in short-term and long-term periods. To assess the impacts of flooding disasters on roadways, various studies have investigated sampled roadway damages with pavement engineering techniques such as a direct damage analysis using cores/bores. In addition, even though existing methods provide a detailed damage analysis of pavement in a particular location for a particular time period, there is still a practical knowledge gap in understanding network-level roadway functional and structural damages after historic flooding as well as assessing flooding impacts on roadways over time. Since each roadway system encompasses several miles of interconnected networks between cities and States in Region 6, a holistic assessment of roadway damages after flooding events not only provides regional roadway damage patterns but also facilitates an integrated roadway recovery and maintenance plan. In addition, evaluating roadway damages by adopting the most accurate and latest flooding data has been rarely conducted in previous studies. Unfortunately, a lack of holistic perspective and long-term investigation on roadway damages caused by floods has resulted in the absence of accurate maintenance cost prediction.

To tackle this demand, this study aims to develop a holistic network-level assessment of flood impacts on pavement structures using the pavement distress data provided by LA DOTD and the city of Houston. The proposed study includes the development and implementation of a holistic network-level pavement damage assessment approach for enhancing durability and service life of transportation infrastructure in metropolitan and rural areas. This proposal also addresses an impending national interest of transportation infrastructure rehab after catastrophic disasters. In particular, the proposed research area closely aligns with the mission of the Center that pursues the two following objectives: (1) Objective 2: Promote sustainability and resiliency of the transportation infrastructure renewal and upgrade; and (2) Objective 5: Enhance the resiliency of the transportation infrastructure in the event of extreme weather events. As the critical mass of Region 6's transportation infrastructure has been severely damaged from recent flood disasters, this study that concurrently involves the pavement management systems of Louisiana and Texas has a significant impact on holistic identification of flood impacts on roadways and integrated roadway damage maintenance of Regional 6's transportation systems. In addition, the expected outcomes from this project would assist not only engineers and decision-makers in the Louisiana Department of Transportation and Development (LaDOTD) and the Texas Department of Transportation (TxDOT), but also Region 6's State administrators in evaluating roadway damage at a regional network level and its long-term impacts after flood disasters. Furthermore, the post-flood pavement damage analysis is essential for Region 6's States for the preparation of the claims made to FEMA Federal Emergency in case of future flooding disaster.

2. OBJECTIVES

The primary objective of this project is to develop a holistic roadway damage assessment method using the flood models and the pavement condition data accumulated over the years. This project also aims to provide a means for Louisiana and Texas (ultimately to all Region 6's States) to intuitively identify roadway damage patterns at the network level caused by flooding over time.

The proposed research objectives have been achieved through the completion of the following tasks: (1) Investigate roadways in Louisiana and Texas damaged by previous flood disasters using the 2016 flood data and FEMA flood maps and the 2017 Hurricane Harvey flood map; (2) analyze pavement assessment data obtained from the Pavement Management System (PMS) in the Louisiana Department of Transportation and Development (LaDOTD), and the city of Houston; (3) incorporate the pavement condition data into the flood models in GIS; (4) evaluate network-level functional and structural pavement damages; (5) develop damage pattern detection and spatial clustering models that indicate space-time pavement damage trends after flooding events; (6) build a prediction model of pavement performance of flood-damaged roadways; and (7) assess pavement damage patterns by comparing with PMS.

Flood events affect various types of pavement distress in short-term or long-term periods after the inundation of roadways. Thus, in this study, the PIs evaluated the impact of flood on roadway pavement in order to find the specific damage pattern. Based on this analysis, the PIs also developed a method to predict the distress scores and pavement performance that can be affected by future flood events.

3. LITERATURE REVIEW

Diverse factors can affect the quality of pavement management procedures: pavement data collection outsourcing; quality of the location referencing data, historical data, consistency, network spatial and temporal coverage; new demands imposed by changing business practices (NCHRP 2009). In particular, in order to develop consistent and accurate multi-year preservation and maintenance plans of pavement systems, their network-level damage analysis reflecting measured condition variables is imperative. In addition, this variation and network-level damage patterns have a significant impact on estimated deterioration of roadways and accuracy of predicted pavement damage (Ruotoistenmäki et al. 2006), providing necessary treatments and budgetary requirements (NCHRP 2009). El-Anwar et al. proposed a mixed integer linear programming model for post-disaster recovery of transportation projects (El-Anwar et al. 2016). Pradhan et al. also utilized geographic information system (GIS) to address disaster management issues (Pradhan et al. 2007), and Karlafits et al. deployed evolutionary algorithms for transportation recovery fund allocation (Karlafits et al. 2007). Recently, numerical prediction models have been widely developed to evaluate the impact of a natural disaster. Advancements in geographic information technology has enhanced the efficiency of these models considerably (Burton 2010). For example, the FEMA's Hazus model provides a feature to determine economic loss from earthquake, hurricane, and flood hazards. These models utilize combinations of data including building stock, economic data, and vulnerability functions (Watson and Johnson 2004).

In addition, the studies conducted by the Louisiana Transportation Research Center (LTRC) clearly illustrate the impacts of Hurricane Katrina on the structure of the roadways (Zhang et al. 2008). The studies utilized diverse devices for the field test including falling weight deflectometer (FWD), ground penetrating radar (GPR), and other direct evaluation methods. These direct assessments showed that the structure of asphalt pavement including the stiffness of both asphaltic layer and subgrade was not significantly affected by flood waters. It also illustrates that the impacts of flooding on concrete pavement were less than asphalt pavement. Due to diverse materials and structures of composite pavements, the conclusion on the direct relationship between flooding events and pavements was not been made (Zhang et al. 2008).

Several studies were also conducted to investigate the impact of flooding disasters on roadway pavement. Chen and Zhang (2014) used PMS data for District 02 before and after the 2005 Hurricane Katrina. In their study they selected IRI (International Roughness Index) and rutting as the criteria for assessing the pavement performance. For highly deteriorated pavement sections they found that the deterioration slope of the IRI in 2005 to 2007 was 10 in/mile greater than the slope in 2003 to 2005, and for rutting, the maximum rut depth in 2007 was at least twice the depth in 2005. It was concluded that the average IRI for flooded asphalt and composite pavements was slightly higher than non-flooded. It was the opposite for concrete pavement in which the average IRI was slightly lower in the flooded zones. The research showed that the rutting depth for asphalt pavements in flooded areas was slightly lower than non-flooded areas. Whereas one in composite

pavement the maximum rutting depth was slightly higher than one in flooded zones (Chen and Zhang 2014).

For estimating the resilience of pavement after sever flood events, the pavement performance is measured with two different road deterioration models (RD), roughness and rutting-based deterioration models (Khan et al. 2017). The models were created by using the Monte Carlo simulation and transition probability matrix (TPM). The analysis was conducted on 27 different road groups at the network level, including three types of road structures (rigid, composite, and flexible), three different traffic loads (low, moderate, and high), and three categories for pavement strength (poor, fair, and strong). The research was conducted in Australia and the required data were collected from the Transport and Main Roads Authority, Queensland (TMR-QLD) database. The database was used for data validation for the RD models. Previous studies revealed that the impact of flooding to the road pavement leads to changes in its roughness (ΔIRI), and these changes are dependent to the flooding probability and the amount of loss in modulus of resilience (Mr). The researchers in this study defined different scenarios based on the probability of flooding in a region, pavement structure, and traffic loading of the road segments. They calculated the pavement's performances for each scenario using the two aforementioned road deterioration models (roughness and rutting-based RD). The proposed indicators to attain the pavement performance in different scenarios were as follows:

1- ΔIRI in Year 1 divided by the percent of probability of flooding (ΔIRI/Pr)
2- ΔIRI in Year 1 divided by the percent of Mr loss at subgrade and granular layers (ΔIRI/MrL)

The scenarios were designed according to the following flood probability: 0%, 50% and 100% probabilities in 1 year period. The results showed that the flexible pavement performance is higher than one of composite pavement at the first year after flooding. But overall, the rigid pavement was selected as the most flood-resilient pavement structure type.

A recent study was conducted in Canada to evaluate the impact of flood in concrete pavements performance. They used the Enhanced Integrated Climate Model (EICM) technique to examine the extreme precipitations on concrete pavement combined with a selection of Historical Climate Data (HCD), and applied them into the AASHTOWare Pavement ME software (Oyediji et al., 2019). AASHTOWare Pavement ME is adopted to evaluate pavement structure, material, traffic loads, etc. and variations in incremental pavement deterioration and its performance (Tighe 2015). Two different pavement designs were considered for pavement structure including (1) a collector design and (2) an arterial design. With flood events, their probabilities, and frequencies, various scenarios have been investigated in this study. In this research, the AASHTOWare Pavement ME Design 2.5.3 tool was employed to model the effect of each scenario on typical collector and arterial Jointed Plain Concrete Pavement (JPCP) structure. This study used the following formula (equation 1) to calculate the percentage of damage ratio based on IRI.

$$\delta_{IRI}(\%) = \frac{IRI_f - IRI_{nf}}{IRI_{nf}} \quad (1)$$

Where δ_{IRI} (%) is the IRI or overall damage ratio, IRI_f is the terminal IRI under RCP 4.5 Extreme Precipitation (EP) or flood conditions, IRI_{nf} is the terminal IRI at base-case or no-flood scenario. They calculated the damage ratio under each scenario (different flood event cycles) for both aforementioned structures (collector and arterial). They found that the arterial JPCP (Jointed Plain Concrete Pavement) had a higher damage ratio compared to collector JPCP for 50-year extreme precipitation, while for a 100-year extreme precipitation it is the opposite. In addition, the damage ratio for a collector road under 100-year extreme precipitation is higher than the arterial.

In addition, one study used Mechanistic-Empirical Pavement Design Guide (MEPDG) to understand the impact of flood events on the road pavement's performance. The MEPDG system is used to predict the pavement performance under various situations (AASHTO 2015). The research was separated into two main parts: (1) a pavement damage analysis due to flooding and (2) flood characteristics and design flood (Lu et al. 2018). In the pavement damage analysis, the following four possible patters were identified:

1- Delayed effect: which indicates that there was no significant affect on the pavement due to flooding and it might have long-term impact.
2- Jump effect: shows the short-term effect of the extreme situation but no long-term impact is identified.
3- Jump and delayed effect: which is a combination of the previous two possibilities that means there is both short-term and long-term impacts for the pavement due to flooding.
4- Direct failure effect: that implies the failure and total destruction of the pavement.

The pavement structure types that were investigated in this research include arterial and collector pavement types. The loss of pavement performance for each structure was calculated based on different situations and scenarios that were attained from a design flood section. For all scenarios it was concluded that a 1-day flood event does not have a visible impact on the pavement performance. In 4-day duration, the damage ratios reach to 0.39% for arterial and 0.46% for collector pavements for all study cycles. It can be concluded that the short-term precipitation does not significantly affect the pavement structure's performance. However, the 22-day duration simulation showed that the damage ratio increases from 0.39% to 1.17%. The research studies in this sphere are conducted through field tests, analyzing the variations in different characteristics of pavement structure, and comparing the conditions before and after the disasters. In this research, the effect of flood on the road pavement performance was investigated in a data-driven holistic level. In addition, a roadway damage pattern was revealed to build a foundation for design a performance prediction method that can help understanding the variations in pavement characteristics after each flood event.

4. METHODOLOGY

The research investigates the impact of flooding (2016 Louisiana flood and 2017 Hurricane Harvey in Texas) on pavement by holistically assessing the accumulated pavement condition data. For severe flood incident in Louisiana in 2016, the PMS data from 2013 to 2015 were considered as the pavement condition data before the event and the PMS data from 2017 to 2019 databases were considered as the post-disaster data. For the 2017 Hurricane Harvey event, the Pavement Condition Index (PCI) scores collected from 2016 to 2018 for the city of Houston were analyzed in this study. The analysis was conducted based on the comparison of the pavement distress data before and after the event. Three different sources of data were available to detect the flooded areas: (1) DOT reports about road closures due to the flood events (The roads in the reports were considered as flooded control sections); (2) the flood feature maps that identify the estimated flood area for each parish; and (3) FEMA high-risk flood areas. The conjunction of each datapoint in the pavement condition data (coordination data defined in PMS for each datapoint) with the areas defined in these feature maps were considered as flood zone control sections.

Therefore, the following three types of analyses were conducted for this study in order to evaluate the effect of flood on road pavements.

1. Simple analysis (mean values) with the different approaches for distinguishing the flooded roads in the selected parishes.
    a. Analyzing the LA DOTD reports to detect the flooded roads and control sections.
    b. Using estimated flood maps to distinguish the roadways where are located in inside of the estimated flood area.
    c. Analyzing the variations of pavement performance before and after the Texas 2017 flood event using the pavement condition data of the city of Houston.
2. Clustering analysis that is divided into the two different analyses.
    a. Single feature cluster analysis, which investigated the statistical characters of a single attribute such as IRI and integrated them with flood zone feature map.
    b. Multiple feature cluster analysis (grouping analysis), which conducted analysis based on several features to find clusters of datapoints with similar statistical characters based on various attributes.
3. Short-term and long-term analyses that investigate the immediate or long-term effects of flood on road pavement.

These analyses facilitate identifying the features/attributes that are effective in evaluating the flooded roadways' distress data. In addition, the distress types that are mostly influenced by flood can be detected. The ultimate goal in this research is to predict the trends and alteration of pavement conditions of the flood induced control sections. Based on the study findings regarding the required attributes, the PIs built a pavement damage prediction model using the two datasets. The first one is a dataset for the attained attributes from before-and-after analysis of pavement condition alteration. The second dataset contains similar attributes but combined with FEMA flood data. In addition, two different prediction models utilizing Support Vector Machine (SVM) and XG Boost (XGB) classifiers were used and their accuracies were compared.

Since the Texas Department of Transportation (TxDOT) considers the pavement condition data as sensitive information and maintains a strict policy to keep their pavement data confidential, the

PIs received the PCI score data from the city of Houston not including the detailed distress types. To build a consistent and robust method of future pavement deterioration affected by future flood events, the PIs employed the detailed and long-term PMS data provided from LA DOTD.

To accomplish the overarching goal of this study, this research followed the tasks.

(1) Collecting Louisiana and Texas flood data from various sources including FEMA high-risk flood zones, and Louisiana's 2016 and Texas 2017 flood data available in ArcMap online: The PIs investigated roadways in Louisiana and Texas damaged by previous flood disasters using the 2016 Baton Rouge and 2017 Houston flood maps. Data for losses caused by a disaster event in a region can be presented by impact assessment models that contain sets of elements reflecting hazard, exposure, and physical vulnerability. Hazard components encompass the physical characteristics of a hazard event.

(2) Collecting pavement condition data and map the coordination of each record to ArcGIS (ArcMap Software) to identify and distinguish data points inside and outside flood areas: The PIs collected the pavement condition data from LaDOTD and the city of Houston. To efficiently analyze an enormous amount of pavement condition data accumulated, the PIs did cleansing and normalization of pavement assessment data.

(3) Incorporating the pavement condition data into the flood models: To identify the pavement damage conditions represented by the Pavement Quality Index (PQI) of flooded roadways according to the historical flood scenarios, the PIs incorporated cleaned pavement condition data (Task 2) into the flood models in GIS (Task 1) based on spatial information.

(4) Conducting short-term and long-term impact analyses: The PIs conducted a simple analysis that includes mean values, variations, standard deviations, etc. on pavement distress and compare the results of datapoints inside and outside of flood areas to find the pavement distress types that were affected by flood events. Short-term and long-term effects of flood on pavement distress were also investigated in this analysis.

(5) Conducting network-level analysis of pavement damages and developing damage pattern detection and spatial clustering models: The PIs conducted a detailed analysis including clustering analysis and grouping analysis to find clusters of datapoints with similar statistical character and find a relation between those data points with flood data. To evaluate functional and structural pavement damages, the network level analysis was conducted by comparing non-flooded (control sections) and flooded sections using statistical techniques, Analysis of Variance (ANOVA), which is the most commonly used technique for comparing the means of groups of measurement data. This technique using the general linear model (univariate) in SPSS software was executed to partition variance observed in a particular variable into pavement damage components. In addition, the PIs applied the abovementioned analysis based on the flood data and compare their results.

(7) Developing a prediction method: The PIs developed a prediction model based on attributes attained from the pavement condition analyses that illustrated the impact of flood on pavement performance. This study built the two different prediction models and compared their accuracies to improve the accuracy of a prediction model for future pavement performance of flood-vulnerable roadways.

5. ANALYSES AND FINDINGS

5.1. Analyses based on the LA DOTD reports for the 2016 flood event

This research investigates the impact of the 2016 Louisiana flood event with the PMS data of the East Baton Rouge parish collected during 2013, 2015, and 2019 years. In the first step, the flooded roads were identified based on the road closure announcements and reports provided by LA DOTD. Road closures caused by flooding in the period of the 2016 Louisiana flood indicate that the roadway sections had been inundated and did not provide a proper service. In total, 24 control sections were selected to be investigated, including 12 control sections considered as flooded roadways and another 12 sections considered as non-flooded roadways. As a next step, the variations in IRI and rutting in pavement structures of these sections were analyzed.

The increase/decrease of distress data were calculated by considering the following assumptions:

(1) Since the PMS data for the year 2016 were collected after the flood, the 2015 PMS data were considered as the distress data before the flood event.
(2) The distress scores in 2016 were considered as the short-term (immediate) effect, and the scores in the following consecutive years (2017-2019) were considered as long-term effects.

The following equations show the short-term and the long-term effect of flood on the selected control sections. Equation 2 shows the calculation of mean values for each year.

$$Mean(X_j) = \frac{\sum_{i=1}^{n_j} X_{i,j}}{n_j} \quad (2)$$

Where X represents the mean value of each type of distress data for each control section, j is the target year, n is the number of datapoints for each control section, and i represents each datapoint in the PMS database. Using the mean values of distress data for selected control sections, the short-term effect of the flood year 2016 can be calculated by equation 3.

$$S_{cs}(X) = \frac{Mean(X_{2016}) - Mean(X_{2015})}{Mean(X_{2015})} \quad (3)$$

Where S_{cs} is the growth rate of distress data in the short-term period for selected control sections.

For calculating the long-term effect of the 2016 Louisiana flood on the selected control sections, equation 4 is used. These equations were used for both flooded and non-flooded control sections. Road maintenance and repairs were also performed for the control sections, and thus, some of them represent lower distress conditions (not in a consistent damage trend and curve) compared to the data collected on the previous year. As a result, the highest mean value of distress between the years, 2017 and 2019, was selected for estimating the growth rate of distress in the long-term period.

$$L_{cs}(X) = \frac{Max(Mean(X_j)) - Mean(X_{2015})}{Mean(X_{2015})}, \qquad 2017 < j < 2019 \quad (4)$$

Where L_{cs} is the growth rate of the distress data in the long-term period for the selected control sections. Table 1 shows the results of this analysis.

Table 1: The short-term and the long-term growth rates of the selected control sections in the East Baton Rouge parish based on the flood inundated roads reported by LA DOTD

Analyzed feature(s)	Flood (S_{cs})	Non-flood (S_{cs})	Flood (L_{cs})	Non-flood (L_{cs})	Comment
IRI	-0%	-2%	+4%	-0%	An increase in IRI can be seen in the long-term assessment of the flooded roads, while the non-flooded roads do not show the increase in IRI.
Alligator cracking	+11%	+3%	+16%	+3%	The increase rate in rutting is significantly higher for the flooded control sections compared to ones of the non-flooded sections in both the short-term and long-term analyses.
Faulting	+279%	+193%	+150%	+139%	Faulting score is highly increased in the short-term and the long-term for both the flooded and the non-flooded control sections, but the flooded roads have the higher increase rate.
Random cracking	+4%	+3%	+4%	+2%	The flooded roads show slightly the higher increase in random cracking in both the short-term and the long-term analysis compared to ones of the non-flooded sections.

The PMS data encompass several abnormal data that can be affected by external variables. For example, the negative growth in IRI can be detected with immediate repair/maintenance work (not showing in the PMS datasets) or can be errors caused by device calibration. Figure 2 shows the selected roadways that were inundated during the 2016 Louisiana flood (highlighted in blue color). Values of the average IRI for each control section in the years 2013, 2015, 2016, 2017, 2018, and 2019 are shown in Table 2 that is divided into the flooded and the non-flooded control sections. Table 3 shows the variations of IRI from 2013 to 2019 for the flooded and the non-flooded roads. ΔIRI is calculated by subtracting each year's average IRI from its previous year (equation 5).

$$\Delta IRI = IRI_j - IRI_{j-1} \quad (5)$$

where, j = year of data collection

Figure 2: The flood inundated roads in the East Baton Rouge parish highlighted by blue color in ArcMap

Table 2: Average IRI for each selected control section in both the flooded and the non-flooded areas

LRS_Flooded	2013	2015	2016	2017	2018	2019
255-02-1-010	67	153	146	145	157	157
254-01-1-010	87	271	292	295	297	292
817-40-2-010	44	166	161	162	165	167
817-09-1-010	72	213	214	224	200	193
013-05-1-010	33	96	86	78	98	95
258-31-1-010	39	119	125	120	124	80
817-20-1-010	81	211	202	203	226	154
454-01-2-010	38	117	120	118	119	121
013-04-2-010	91	62	70	72	73	74
258-33-1-010	67	174	179	175	181	172
257-04-1-010	40	109	97	110	115	114
258-02-1-010	67	193	189	192	199	199
Flooded_Avg	**61**	**157**	**157**	**158**	**163**	**152**

LRS_NonFlooded	2013	2015	2016	2017	2018	2019
007-08-1-010	22	89	103	107	106	115
414-01-1-010	38	107	109	116	105	110
450-10-1-010	39	125	121	120	117	125
007-90-2-010	75	162	157	172	163	137
060-01-1-010	89	214	201	191	194	201
077-05-1-010	85	230	218	227	231	234
250-01-1-010	50	131	137	130	111	117
254-02-1-010	57	158	156	143	138	141
258-32-1-010	88	249	235	264	225	218
255-01-1-010	74	219	209	192	217	222
414-01-1-010	38	107	109	116	105	110
450-92-1-010	61	188	194	194	186	186
NonFlooded_Avg	**60**	**165**	**162**	**164**	**158**	**160**

Table 3: Variations in average IRIs from 2013 to 2019 for the flooded roads

Year	Average IRI (Overall)	ΔIRI (Flooded)	ΔIRI (Non-Flooded)
2013	60.08	-	-
2015	160.98	96.34	105.45
2016	159.52	-0.20	-2.71
2017	161.07	1.16	1.93
2018	160.41	4.81	-6.12
2019	155.53	-11.17	1.41

This study considered the average IRI for 2016 as the roadways' roughness index affected after the 2016 Louisiana flood incident. The overall average of IRI in 2013 is significantly different from the other years, and thus, it was excluded from the IRI variation calculations (shown in Figure 3b). Figures 3(a) and 3(b) show the variations in average IRI and ΔIRI from 2015 to 2019. Figure 4 shows a significant drop in IRI of the flooded roadways after the flood event.

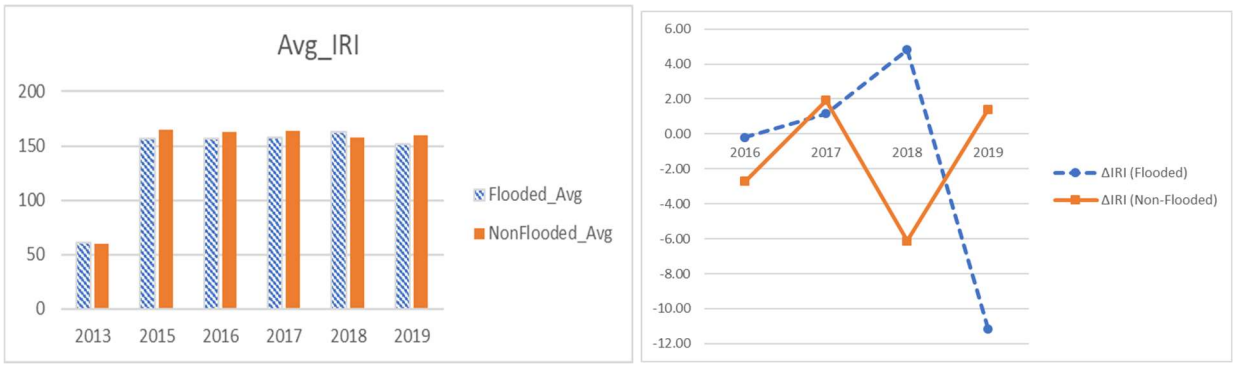

(a) (b)

Figure 3: (a) comparison of average IRIs during 2013 to 2019, (b) variations in ΔIRI for each year from 2013 to 2019

As shown in Figure 3, there is no significant pattern in the variations of average IRIs in the flooded or the non-flooded areas during the surveyed periods. According to the detected PMS data, several decreases in the IRI scores can be analyzed, which are abnormal pavement condition data. Although several previous studies confirmed that flooding does not have considerable effect on pavement, an increase in average IRI is expected since pavement performance is deteriorated over time.

Similar to the IRI comparison analysis, the same method was utilized for analyzing the flood impacts on pavement rutting. Figure 4 and 5 show the measurement data of rutting in the selected control sections during the years from 2013 to 2018. This task includes comparison of the average variations in each consecutive year for the flooded and non-flooded control sections.

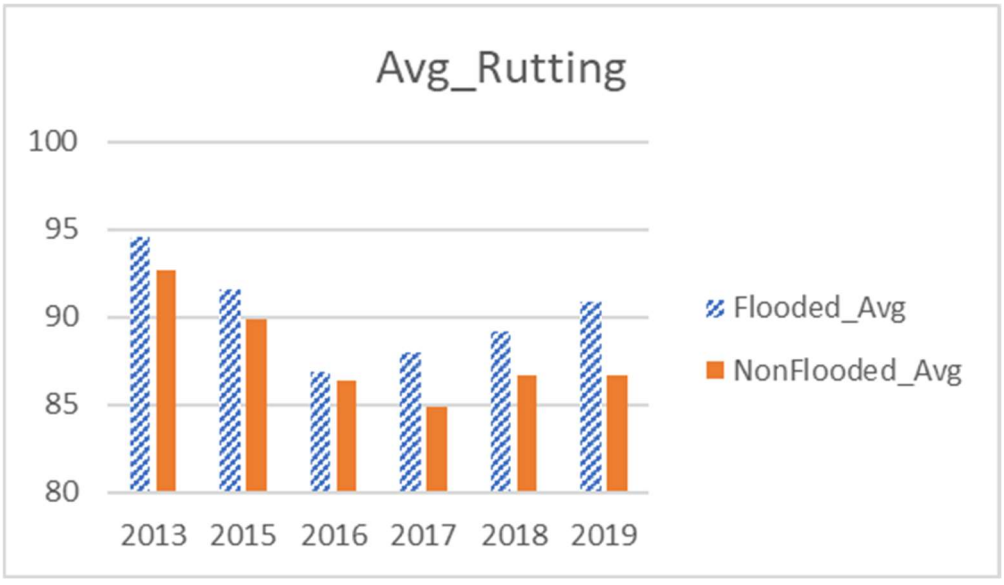

Figure 4: comparison of average Rutting data from 2013 to 2019

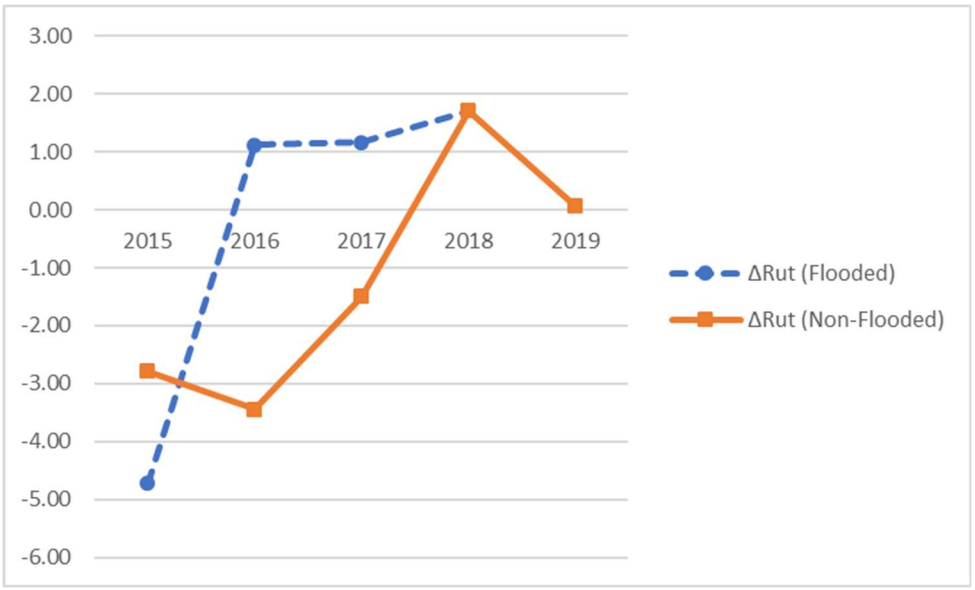

Figure 5: variations in ΔRutting for each year from 2015 to 2019

A significant decrease in rutting measurement in 2016 (the year of the flood event) is evident from Figure 4 and 5. Although Figure 5 shows an increase in the rate of the rutting score in 2017, by comparing the increase of ΔRut in the non-flooded control sections, no conclusion can be made.

In this step, the analyses were conducted on 24 flooded and non-flooded control sections selected in the East Baton Rouge Parish. To identify the latent reasons leading the unexpected results and inconsistent data patterns, the PIs examined any possibility of inaccuracy in data collection and analyses and revealed the possible factors or external variables affecting pavement conditions. First, it is possible that the roadways identified as flooded in the LA DOTD report in 2016, were not entirely flooded, but the entire roadways were closed due to a partial flooded section of the road. Second, the LRS_IDs are found based on the road's name and address in the report. There might be possible errors in mapping some of the LRS_IDs according to their addresses. Third, it is also possible that the PMS data contain errors in data collection processes such as issues in a vehicle or a measurement device. According to Dawson (2012), the PMS data contain errors which are difficult to be identified and addressed. These errors can be derived from the data collection system, seasonal changes, human error, the evaluation strategy, the location reference system, etc. (Dawson 2012). Last, since pavement condition data can be captured in different parts of the same control sections, which can produce heterogeneously altered condition data. The first two abovementioned issues could be addressed by using the flood zone maps provided by FEMA, USGS, etc. to separate the flooded areas with the non-flooded ones. The next section includes the details of the PMS data analyses based on the flood zones using the ArcMap software.

5.2. Analyses based on Texas 2017 flood maps

Hurricane Harvey, which is a category 4 storm, occurred in August 2017 that caused a total estimated destruction of $108 billion with at least 82 number of casualties in Texas (Moravec 2017). To investigate the impact of Hurricane Harvey on pavement performance, the PIs selected

the city of Houston for the scope of this study for Texas. During this disaster period, the rainfall continued for about six days causing major flooding and road closures in the city of Houston. Figure 6 shows the intensity of the rainfall in the regions affected during Hurricane Harvey.

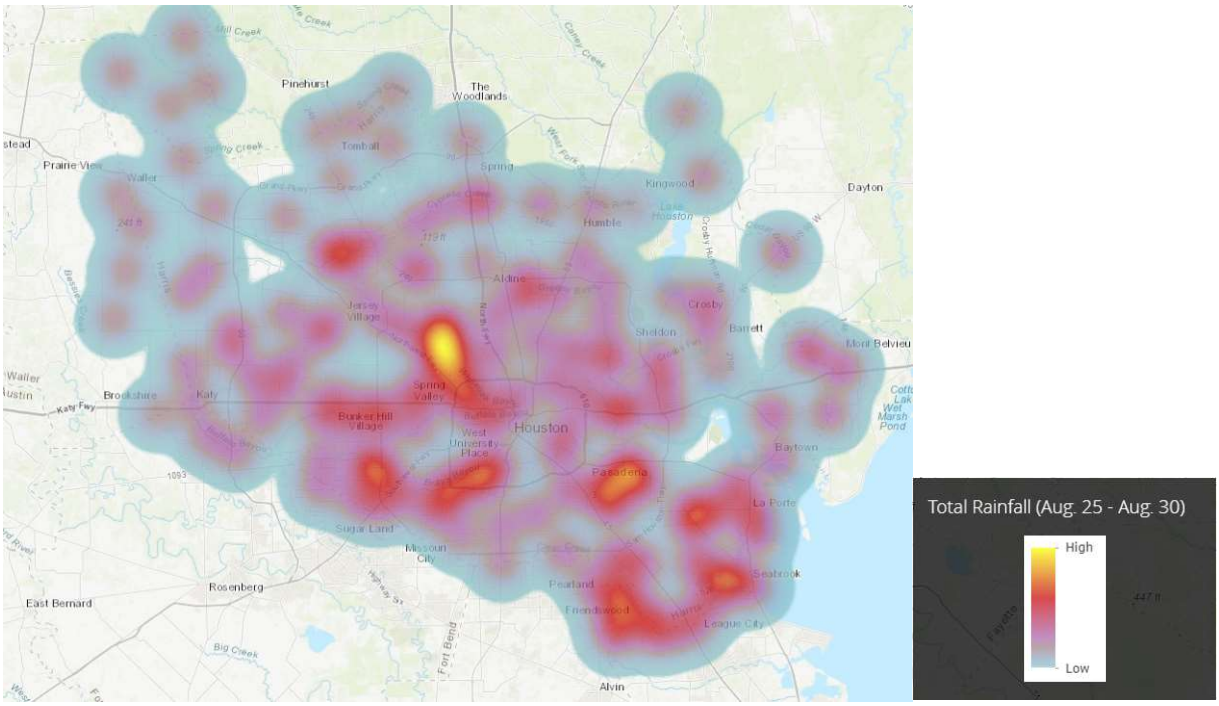

Figure 6: The intensity of the total rainfall in the city of Houston, Texas during Hurricane Harvey (ArcGIS 2017)

Figure 6 shows that there was a heavy rainfall in the central parts of the city, which resulted in a higher rainfall depth than ones in other areas of the city. With the flood map, the inundated roads were identified and stored as an ArcMap Online layer package (ArcGIS 2020) as shown in Figure 7.

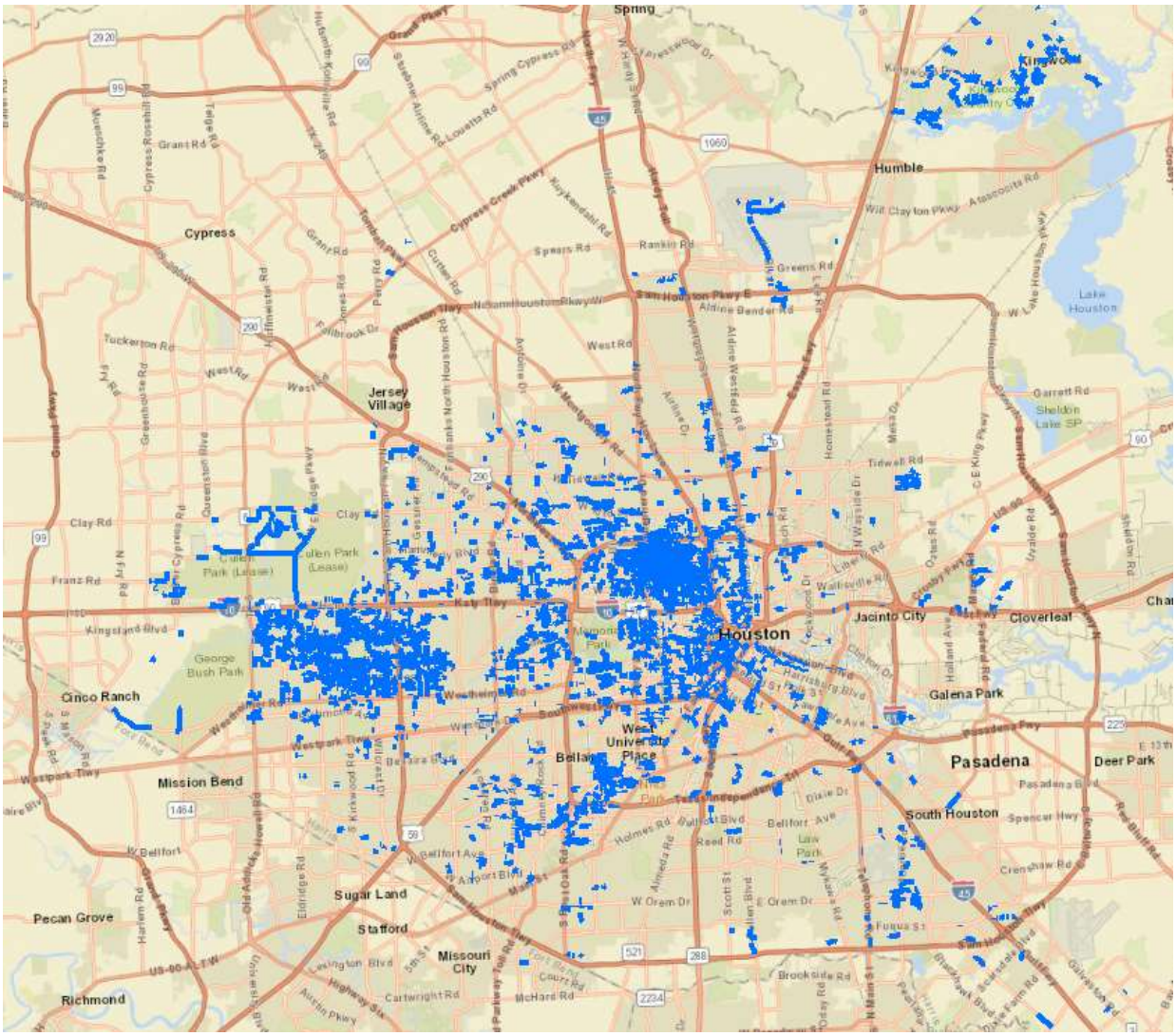

Figure 7: The flooded roads in the city of Houston, Texas, during the Hurricane Harvey

As evident from Figure 7, most of the roads in central parts of city of Houston were inundated during the event, which are the corresponding results (heavier rainfall areas) shown in Figure 6. The Pavement Condition Index (PCI) scores in the years before and after the hurricane i.e. 2016 until 2018 were provided from the city of Houston and analyzed for this study. The PCI is calculated based on a numerical index between 0 and 100 to show a pavement condition. To investigate the impact of the flood on pavement in the city of Houston, the study compared the performance behavior of the flooded and the non-flooded pavement before and after the flood occurrence. Figure 8 shows the analysis of this comparison.

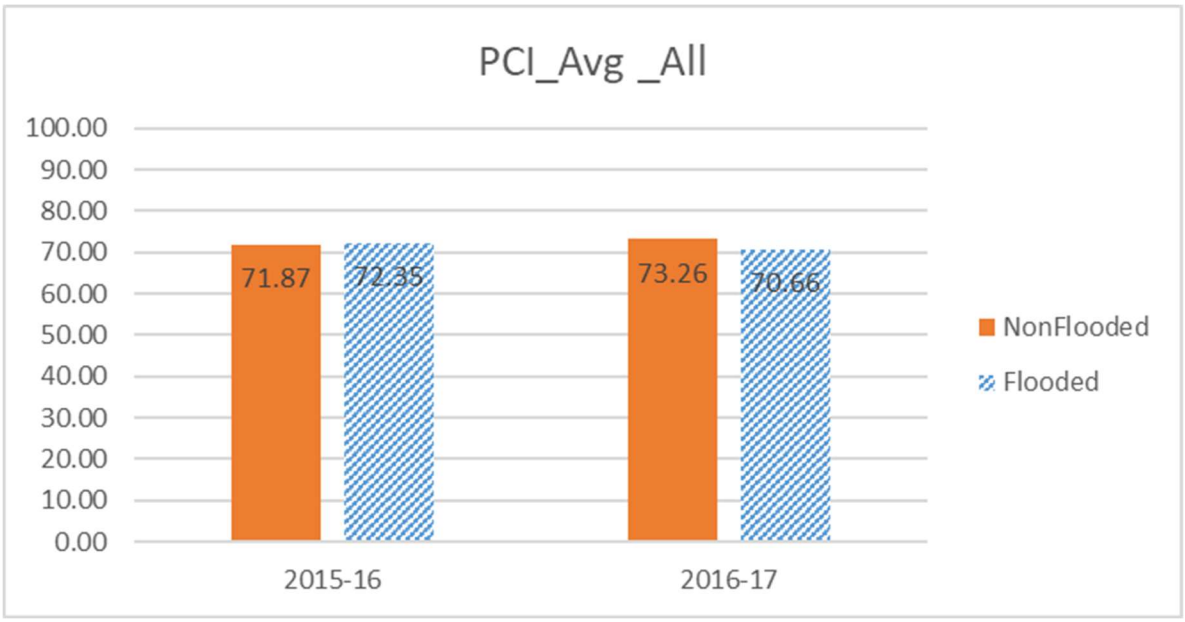

Figure 8: Comparison of variations of pavement condition index between years in flooded and non-flooded pavements

The increase in the PCI scores, which is the abnormal data, can be considered as a result of repairs and maintenance of pavement during this event that are not shown in the PCI dataset. Figure 8 shows that the PCI scores of the flooded areas slightly are dropped by about 2 percent.

In addition, to improve accuracy of the analysis, the PIs investigated the effect of flood based on the pavement areas categorized with high, medium, and low traffic of roadways. The Annual Average Daily Traffic (AADT) for the city of Houston was mapped into the ArcMap software. Figure 9 shows the mapped results. Each point in Figure 9 indicates a station for traffic count and contains the data about the traffic load of the road it is assigned to. These stations were then complied with flood maps (the blue zones) to distinguish the traffic data of the flooded roads from the non-flooded roadways.

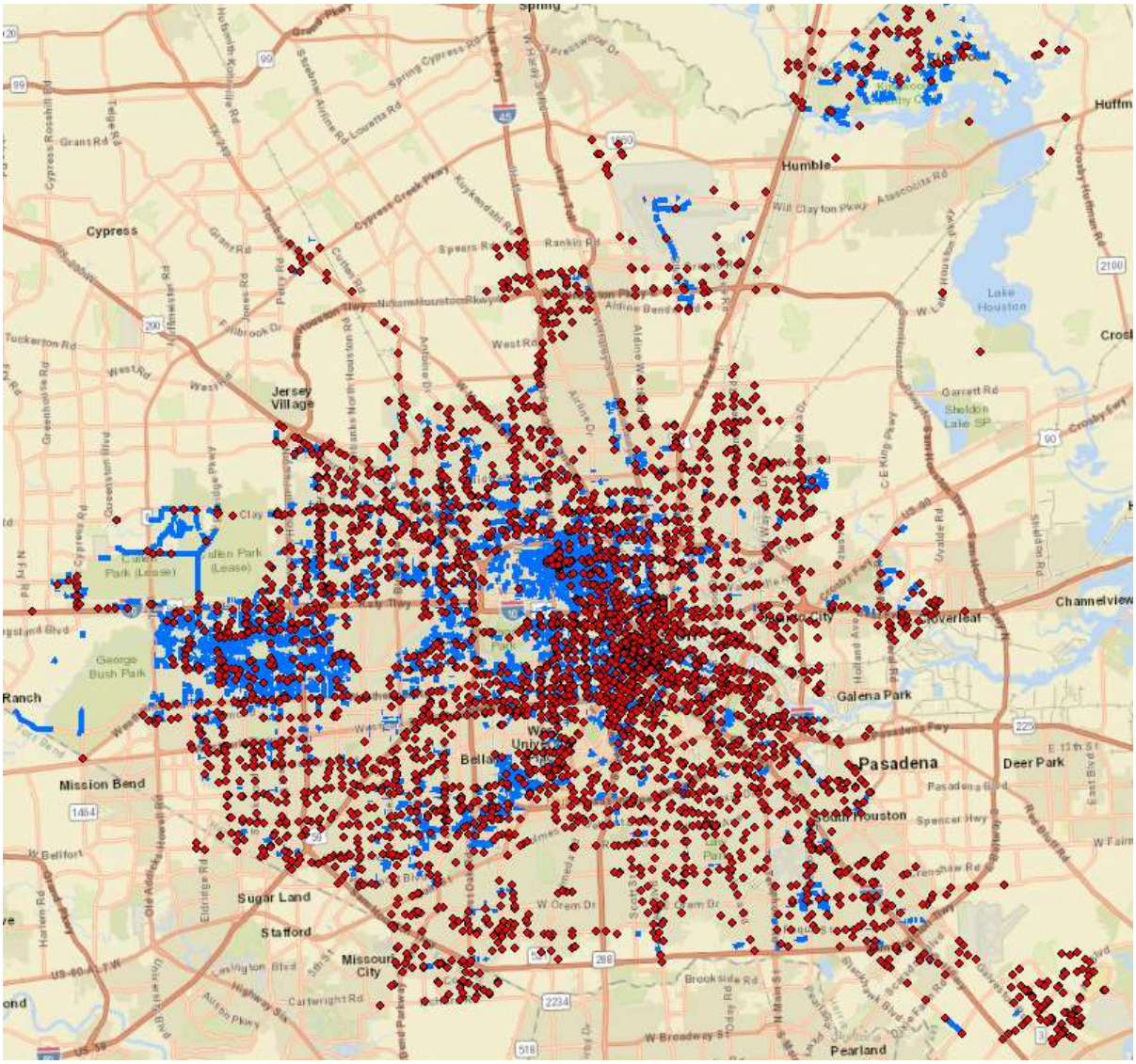

Figure 9: AADT data mapped to ArcMap and complied with the flooded areas

The traffic load was divided into the following three categories: high (above 50,000 traffic volume), medium (between 10,000 and 50,000), and low (below 10,000). The results of the pavement performance analysis according to the categorization based on traffic data are shown in Figure 10.

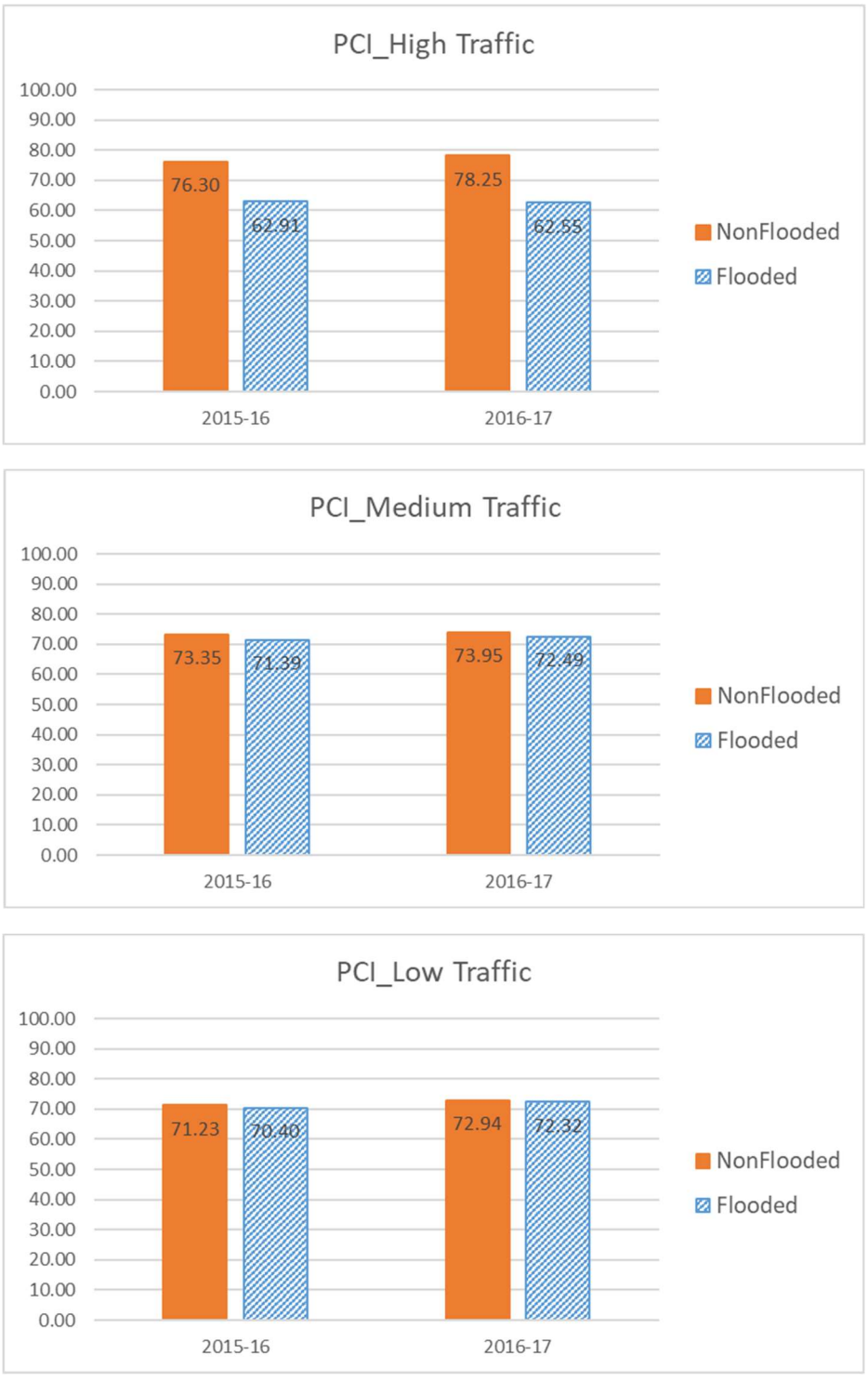

Figure 10: The results of the analysis of pavement performance based on the traffic data categorization

The comparison analysis of the pavement performance of roadways categorized by high, medium, and low traffic shows that the effect of flood on different categories of traffic volume is not significant. The top left chart in Figure 10 shows a considerable drop in PCI of the flooded roads in the high traffic areas. However, since this drop is also evident in the year before the flood (2015-

16), this analysis cannot indicate that flooding significantly affects pavement performance of high traffic roads.

The PIs also examined the flood impact on pavements according to types of pavement: Two major types of pavements, asphalt and concrete, were utilized to classify the affected roadways. The PCI of each type in the flooded and the non-flooded roads were investigated and compared as shown in Figure 11. This outcome shows that the roadways with asphalt pavement were affected by flood, while the Portland Cement Pavements (PCC) performance increased after the year of flood occurrence.

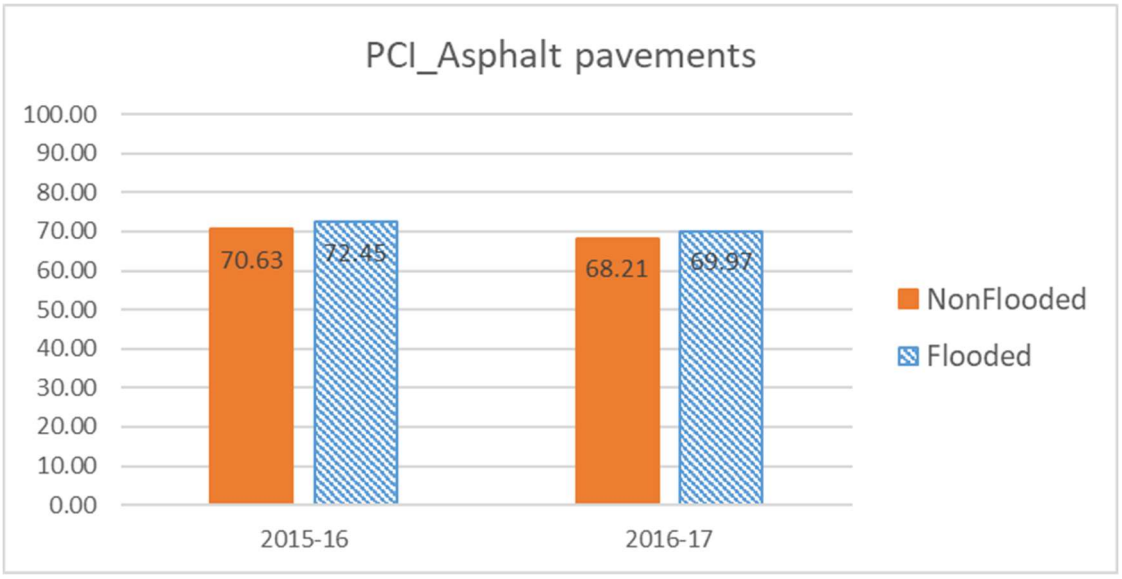

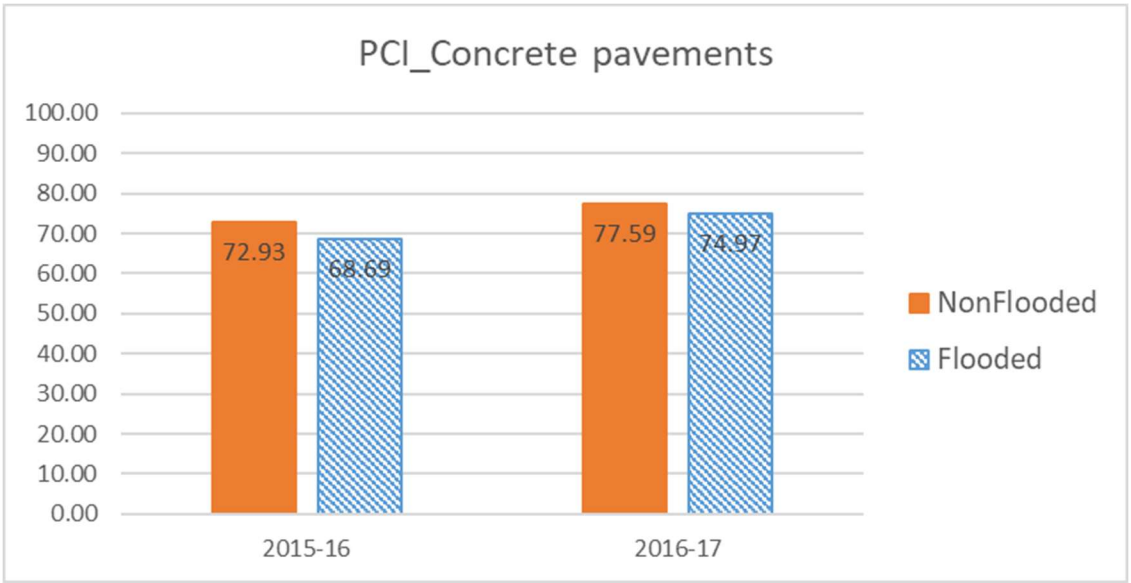

Figure 11: The performance of roadways categorized with pavement types damaged by the 2017 Texas flood

The PIs also classified the roadways based on types of roads: residential/local and major collectors. The effect of flood on pavement performance was investigated on each type separately as shown in Figure 12. There was no significant effect of flooding for residential/local roads in the left hand side of Figure 12. The right hand side of Figure illustrates that the performance of major collectors has been considerably dropped. For both the flooded and the non-flooded collectors, about 5 percent has been dropped.

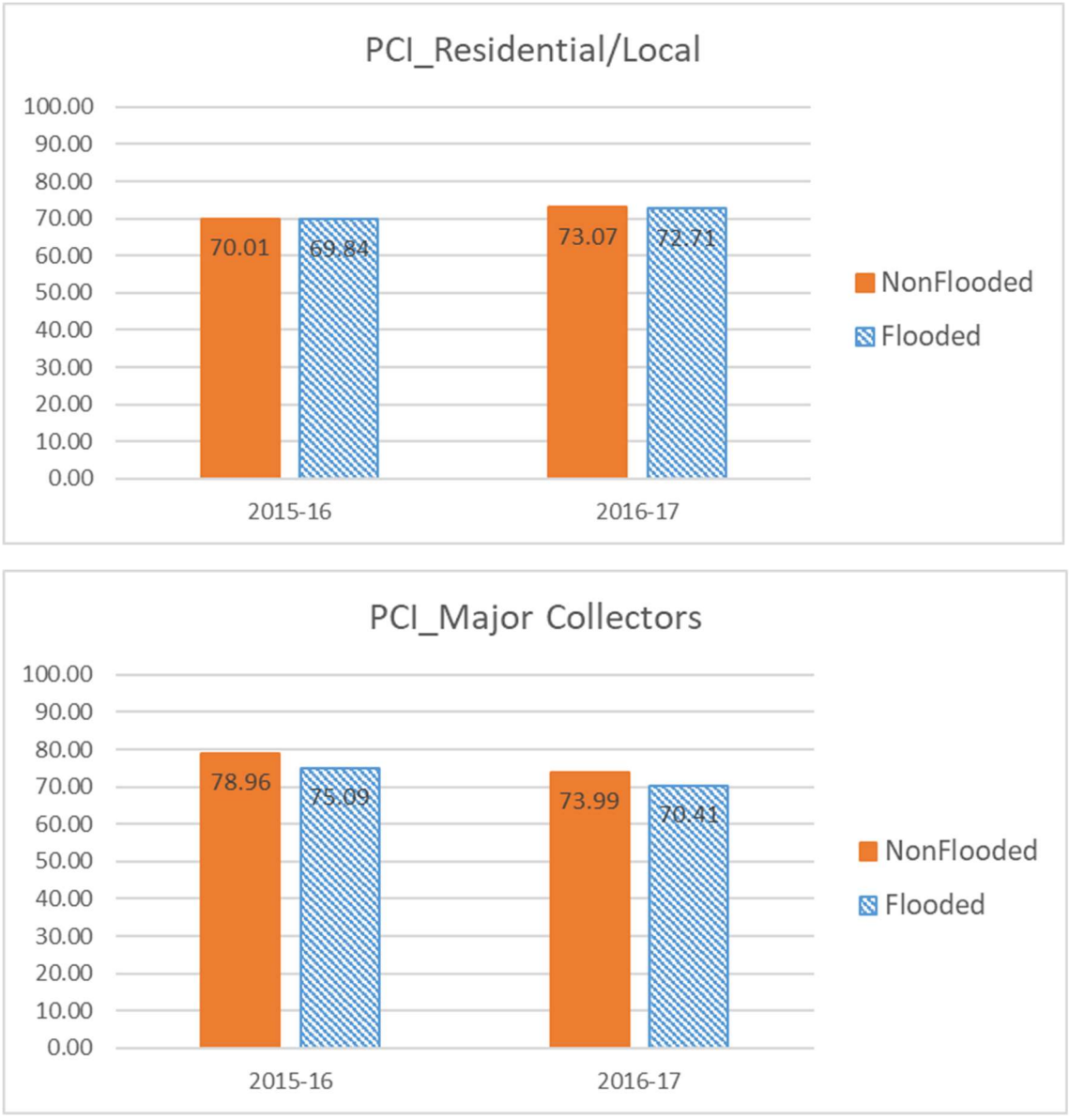

Figure 12: The analysis of the effect of flood on the performance of each road type in the 2017 flood event in Houston

5.3. Analysis based on the Louisiana 2016 estimated flood zones

The PIs conducted the data analysis to examine the impact of the 2016 Louisiana flooding on the following eight parishes by using a PMS database that contains the distress data from 2013 to 2019. (Figure 13):

1. Vermilion parish
2. St. Landry parish
3. Evangeline parish
4. St. Martin parish
5. Iberia parish
6. East Baton Rouge parish
7. St. Helena parish
8. Lafayette parish

The flood maps in the ArcMap software for the Louisiana parishes are based on (1) FEMA and (2) the Louisiana 2016 flood event. Figure 13 shows the 2016 estimated flood map for the selected parishes. The total number of data points in these eight parishes were 26,330. Among the data points, 7,512 points were inside of the high-risk flood area according to FEMA flood maps and 9393 data points were inside of the flood area according to the 2016 flood data. This study used both maps and separately evaluated the statistical behaviors of the flooded roads according to the PMS data.

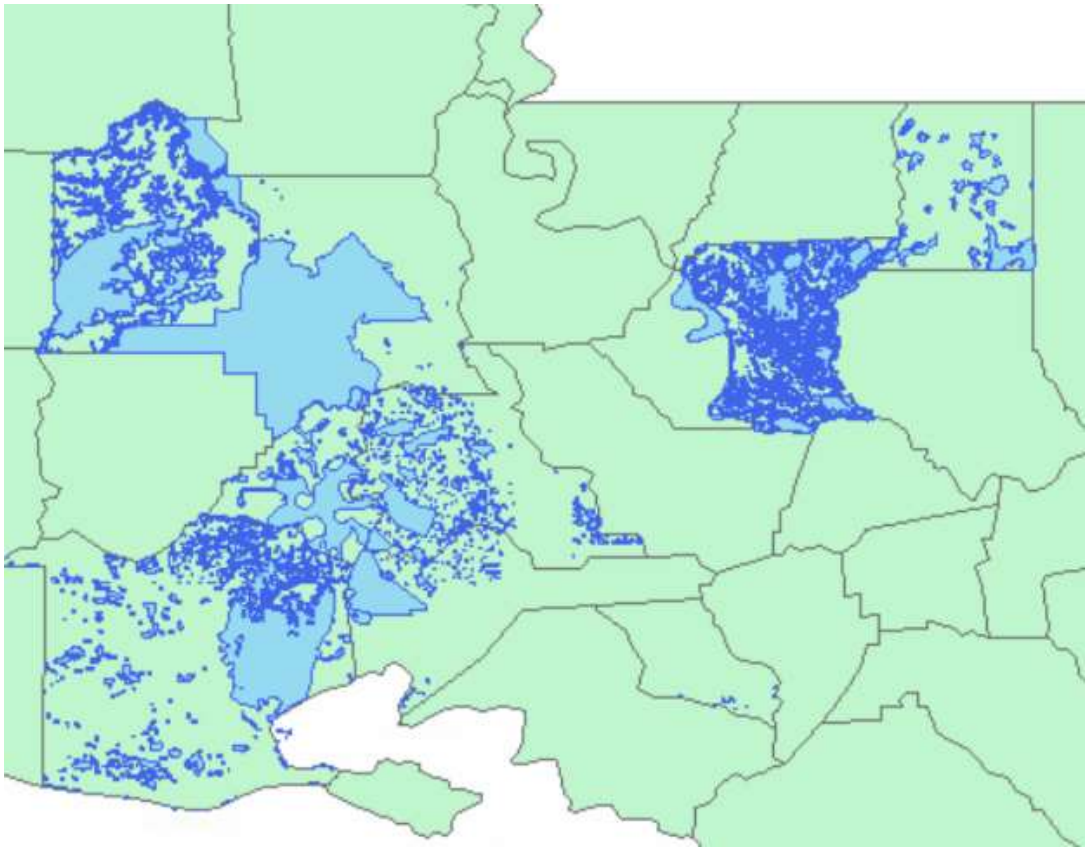

Figure 13: FEMA flood map of the selected parishes

Using the 2016 flood maps, the flooded and the non-flooded roads were separately identified. Figure 14 shows the Lafayette parish as an example that illustrates the process of this separation and is used to conduct the clustering analysis. Using the ArcMap software, the feature map of the flood hazard area (Figure 14a) was applied on the parish and the PMS records representing the location of each data collection point was also mapped (Figure 14b). The conjunction of each datapoint with the flood zone map (Figure 14c) was considered as the flooded and the ones without any conjunction (Figure 14d) were considered as the non-flooded datapoints.

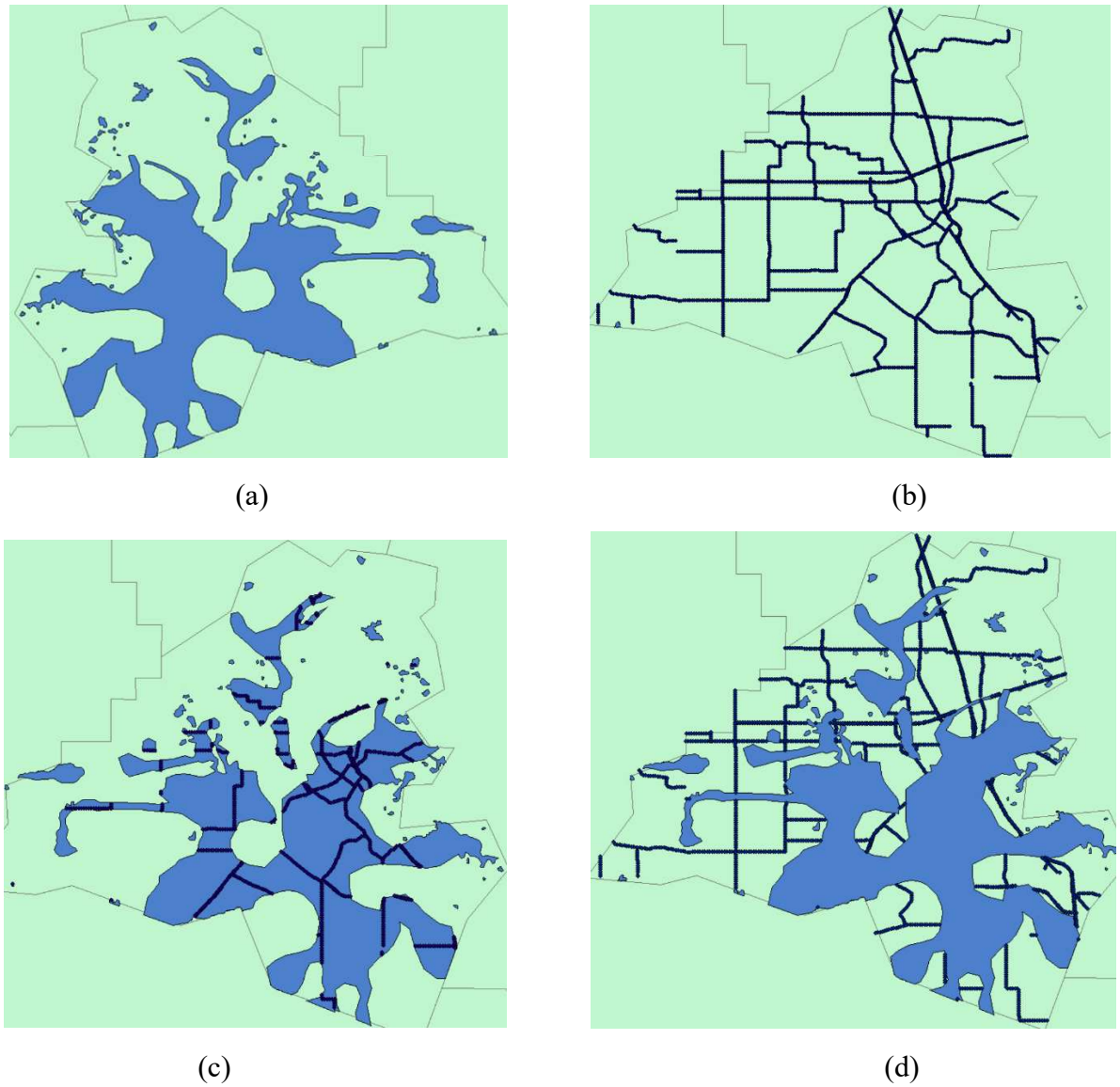

(a) (b)

(c) (d)

Figure 14: The example of the flood zone in the Lafayette parish and the PMS data in ArcMap

Figures 14c and 14d show the PMS datapoints distinguished according to the flood zones. The following distress types and pavement performance indicators were analyzed in this analysis step:

- Alligator cracking (ALCR)
- Average IRI (AVG_IRI)
- Average Faulting (FALT_AVG)
- Performance Index (PERFINDEX)
- Random Cracking (RNDM)
- Roughness (RUFF)
- Rutting (RUT)

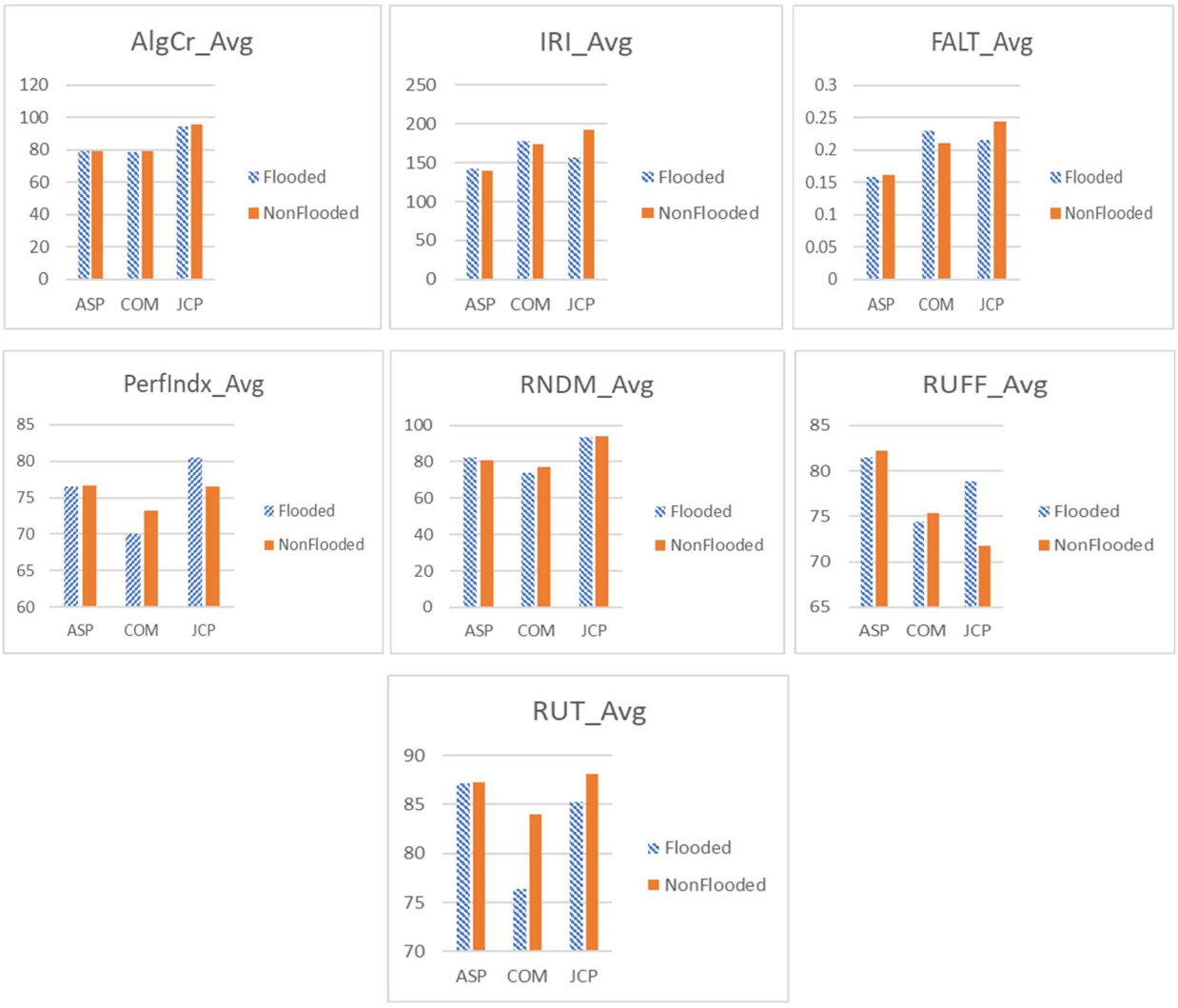

Figure 15: Comparison of distress data between the flooded and the non-flooded areas in the Lafayette parish

Composite pavements show lower average distress scores in rutting, roughness, performance index, and alligator cracking as shown in Figure 15, but they have higher average of faulting and IRI score as shown in the comparison of roads inside and outside of the flood zones. However, there was no significant variations identified in other pavement types.

5.4. Clustering analyses

Investigating the clustering and trends of the datapoints with higher/lower average or standard deviation in a specific zone is vital to understand hidden interrelationships of pavement and other relevant aspects. This analysis illustrates the zones that contain several points with high range of IRI score, or a significant drop or increase in IRI in a part of a road. The cluster analysis for Average IRI was also applied in the ArcMap. The purpose of this clustering using the attained standard deviation attribute was to determine whether the data points with higher variations in IRI are clustered or dispersed. If clustered, we can illustrate in what regions they exist and how close they are to flood zones. Figure 16 shows the clustering analysis applied on the ArcMap based on standard deviation of IRI for each datapoint. The clustering method used in this analysis is called "Anselin Local Moran's I". This analysis was performed with the data of the Lafayette parish.

The PMS data for the Lafayette parish showed that the three types of pavement were used in the roads' structures (1) Asphalt pavement (ASP) (2) Composite pavement (COM), and (3) Jointed concrete pavement (JCP). The distress analysis was conducted for each pavement type.

Along with the mean, the standard deviation of the distress data is calculated separately for the flooded and the non-flooded control sections to investigate the effect of flood in the dispersion of distress values. The Louisiana flood disaster occurred in 2016 and the distress data selected for the analysis are from 2015 to 2019. Higher standard deviations indicate higher variations in the collected data during the years before and after the flood event. The comparison of standard deviation between the flooded and the non-flooded roads can be an indicator for evaluating the flood's long-term impact to the pavement. The following figures show the analyzed distress data for each pavement type.

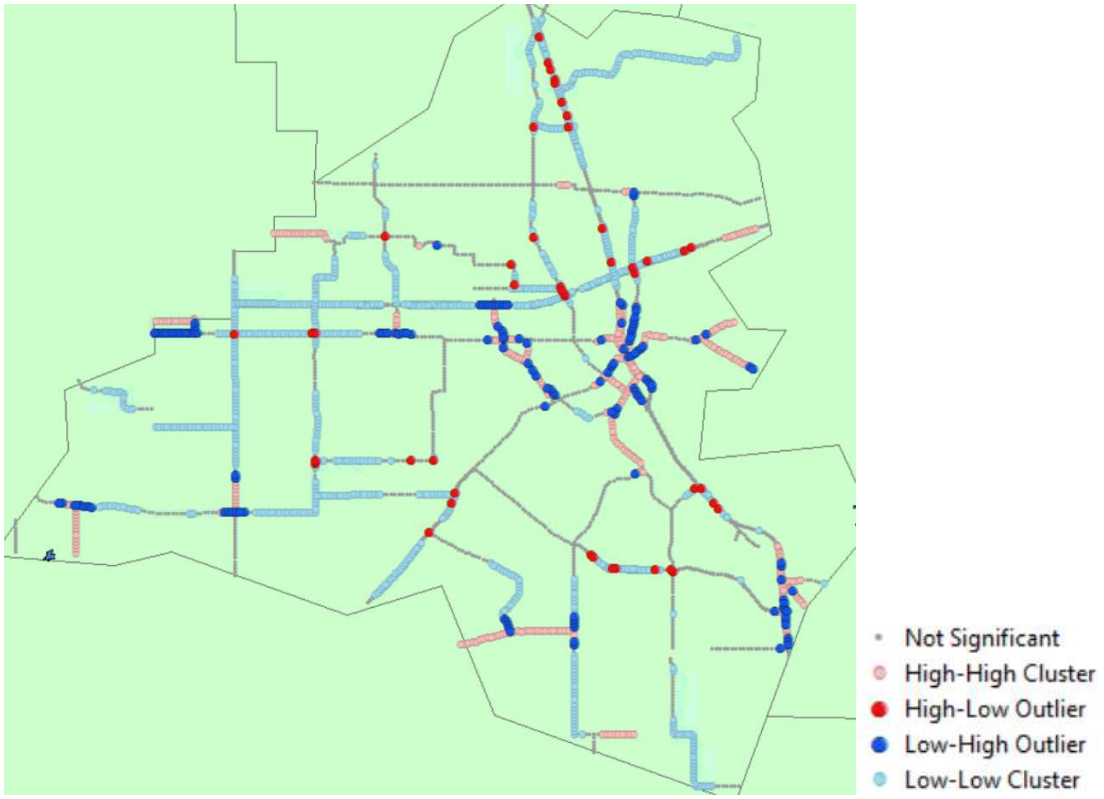

Figure 16: The cluster analysis according to variations in IRI

The color codes in Figure 16 are described as follows:

- The grey points are points that did not show any significant clustering.
- High-high clusters are datapoints that have high IRI deviations near each other.
- Low-low clusters are exactly the opposite of high-high clusters, reflecting the datapoints with low variations in IRI in an area.
- High-low outliers are data with high variations in IRI but are surrounded by datapoints with low IRI variations.
- Low-high outliers on the opposite are data points with low variations in IRI but exist in an area with datapoints that have high values of IRI deviation.

By applying the flood zone of the Lafayette parish to the cluster analysis, the PIs identified and compared each clustering category based on flooded and non-flooded areas as shown in Figure 17.

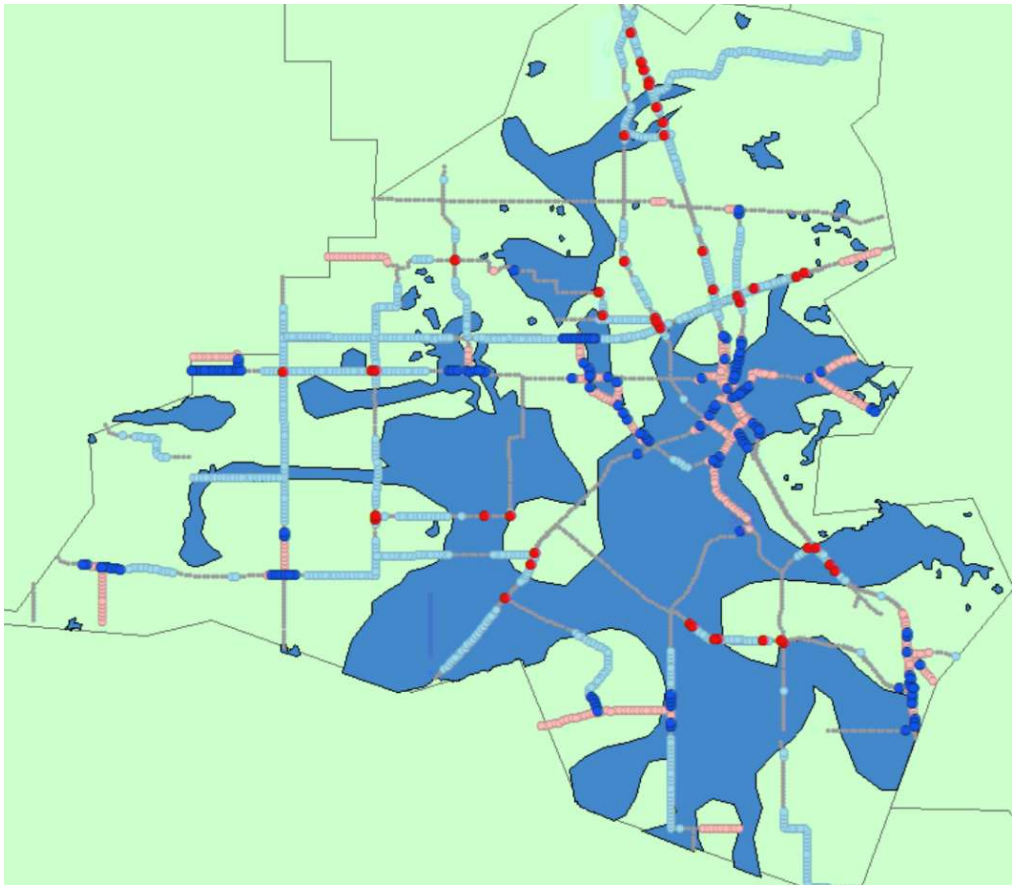

Figure 17: Compliance of cluster analyses and flood zones

The same analysis was applied with other features with the same color codes. Figure 17 shows the clustering of Standard deviation of IRI for the Lafayette parish. Other features such as Variance or Mean values for other pavement deterioration types or performance indicators can be investigated using the clustering and outlier analysis in ArcMap. Figure 18 shows the clustering results of ArcMap based on various features.

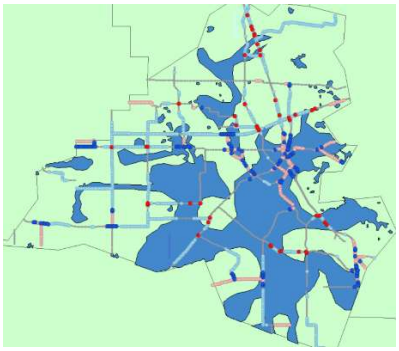

Standard Deviation (IRI)

Variance (IRI)

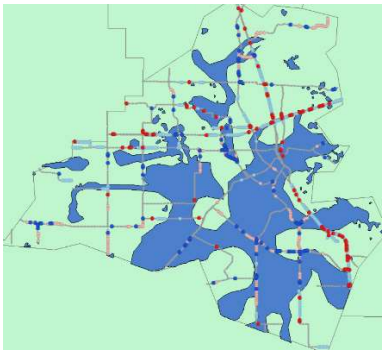

Mean (IRI)

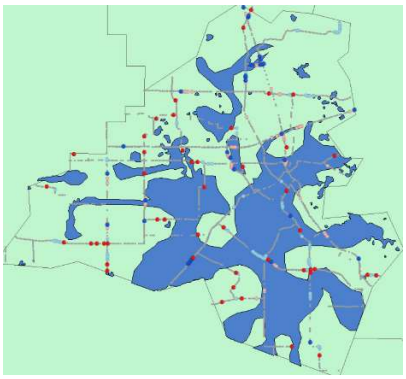

Standard Deviation (Faulting)

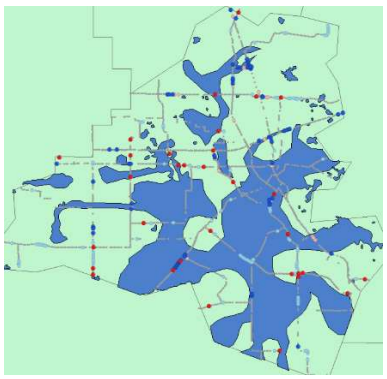

Variance (Faulting)

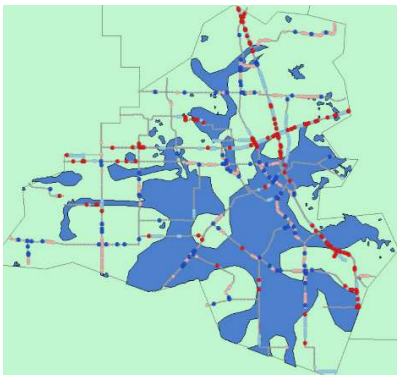

Mean (Faulting)

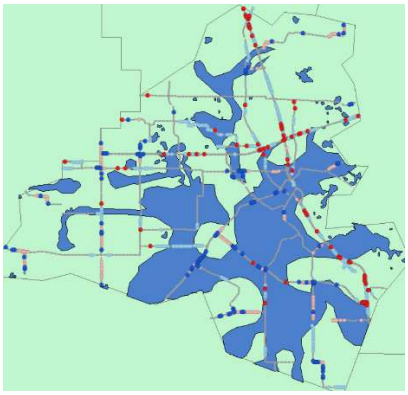

St. Deviation (Performance Index)

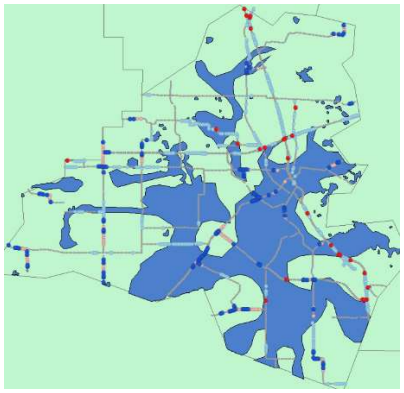

Variance (Performance Index)

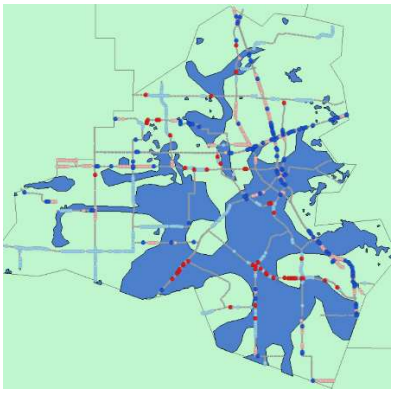

Mean (Performance Index)

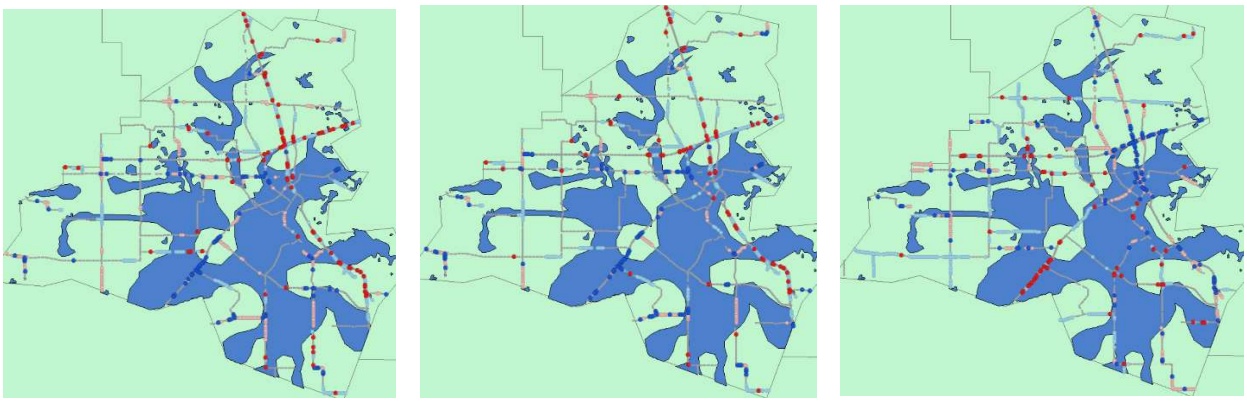

St. Deviation (Random Cracking) Variance (Random Cracking) Mean (Random Cracking)

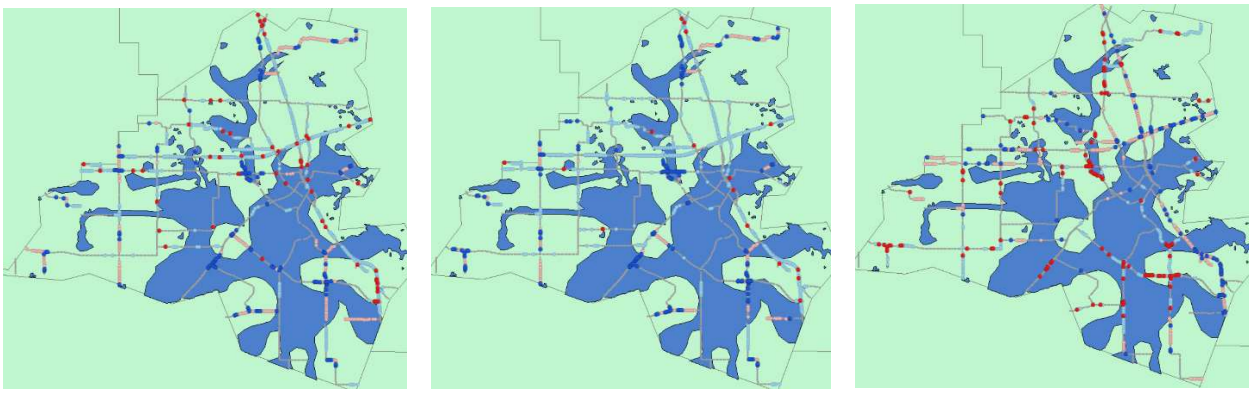

St. Deviation (Roughness) Variance (Roughness) Mean (Roughness)

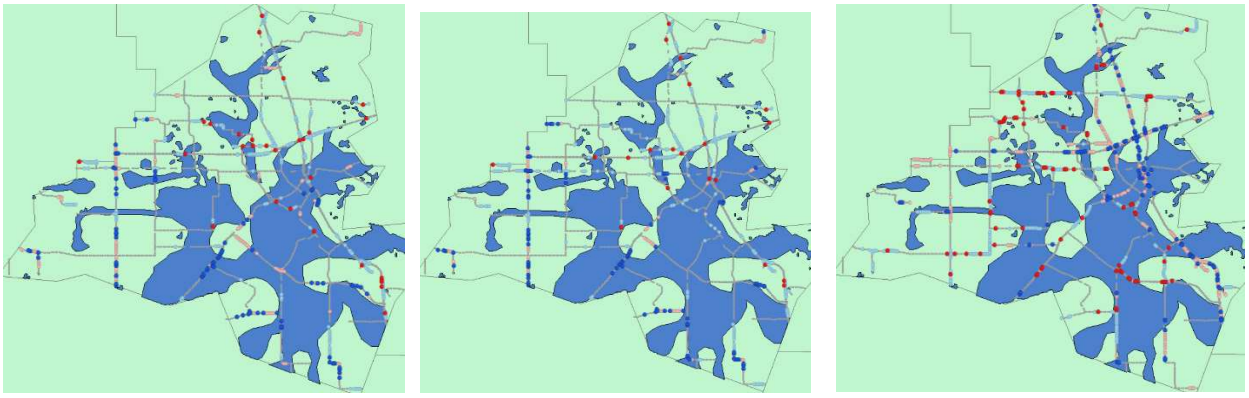

St. Deviation (Rutting) Variance (Rutting) Mean (Rutting)

Figure 18: data clustering and analysis for each pavement deterioration type in Lafayette parish

The clustering analysis was conducted for all of the selected parishes. Figure 19 shows the clustering analysis for pavement performance index.

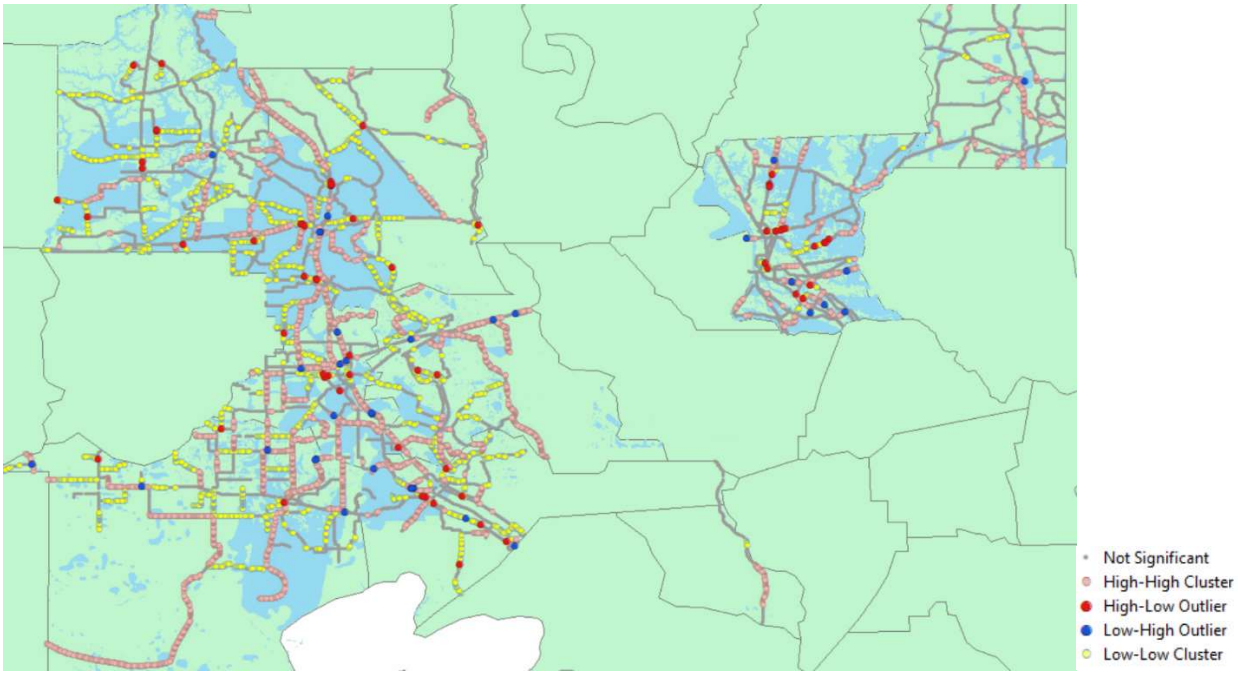

Figure 19: The clustering analysis on pavement performance index for all selected parishes

In Figure 19, pink and red points show clusters of data points with high performance index which are 4,786 in total, and yellow and blue points show the clusters of data points with low performance index which are 3,372 in numbers. Among all the significant data, 37% of data points of high clusters were inside the flood area, and for data points of low clusters, 45% were inside the flood zone. This shows that the low clusters of pavement performance have the majority of significant data inside the flood areas.

The PIs also analyzed statistical characters of several attributes such as pavement distress type, location and elevation, pavement types, etc. using the K-means clustering method. Figure 20 shows three clusters of road control sections using the attributes Pavement type, Flooded/Non-flooded, Elevation, Standard deviation, and Mean.

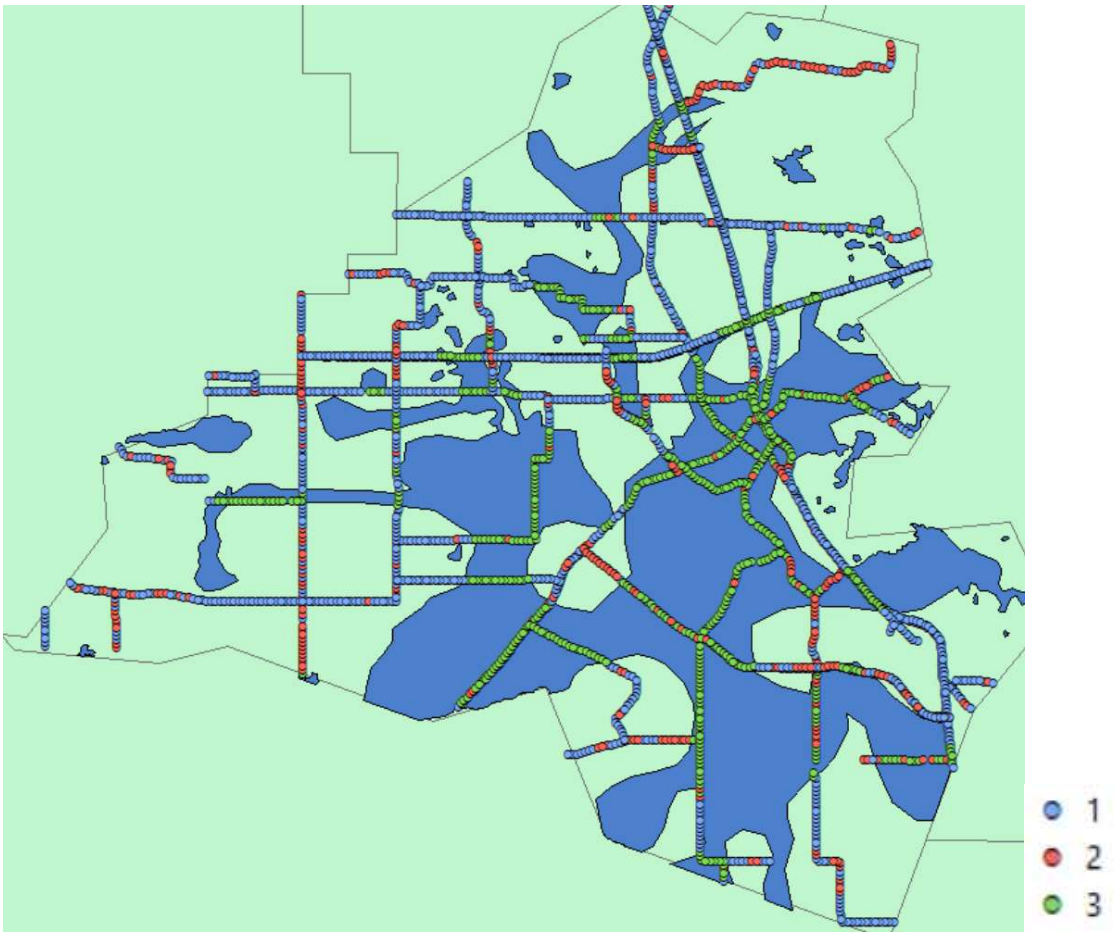

Figure 20: Three different clusters according to pavement type, flooded/non-flooded, elevation, standard deviation, and mean

The number of groups can be assumed based on variations in the Mean value of Pseudo F-Statistic (that shows the distance between all clusters). A huge drop or increase in the grouping mean value, indicates the best group numbers. Figure 21 shows the Pseudo F-Statistic analysis and indicates a significant increase in the mean value from the two (2) number of grouping to three (3) number of grouping (red rectangle).

Pseudo F-Statistic Summary

Number of Groups	Mean	Minimum	Maximum	Median
2	700.6652	664.0099	712.9326	712.8735
3	820.3357	791.7845	839.3639	839.3625
4	862.8298	816.0809	880.7235	880.7235
5	827.1494	710.6409	854.5676	854.5550
6	810.2012	736.0202	863.7018	793.4456
7	804.6923	733.1327	835.6368	835.1417
8	781.5932	704.1012	804.5155	792.5240
9	768.1627	753.9571	779.2844	768.0690
10	746.9665	713.6441	756.4908	752.9440
11	720.7938	671.1590	749.0072	722.5337
12	707.3306	679.7574	726.8976	709.1617
13	693.9173	636.9719	728.3301	701.0589
14	701.9298	681.8765	728.3593	700.8917
15	691.5051	647.7935	713.5126	699.5241

Figure 21: Pseudo F-Statistic summary

As a next step, the PIs conducted a parallel box plot analysis shown in Figure 22. The vertical axis of the plot represents the attributes/features that were selected for grouping analysis. The selected attributes are as follows:

- NonFl_0: indicates flooded or non-flooded roads based on each data point's compliance with the estimated flood zone map. The value 0 is assigned to points that are outside of the flood zone, and 1 is assigned to the points that are inside the flood zone.
- VFrom_GPS: elevation of each point
- Type: pavement structure type, which in this parish is consisted of Asphalt (replaced with 1 in the dataset), Composite (replaced with 2 in the dataset), and Joint Concrete Pavement (replaced with 3 in the dataset).
- MEAN: the mean value of the collected IRI score from 2015 to 2019 for each point.
- STDEV: the standard deviation of the collected IRI values during the years 2015 to 2019 for each point. This indicates the amount of variation of the IRI score for each datapoint.

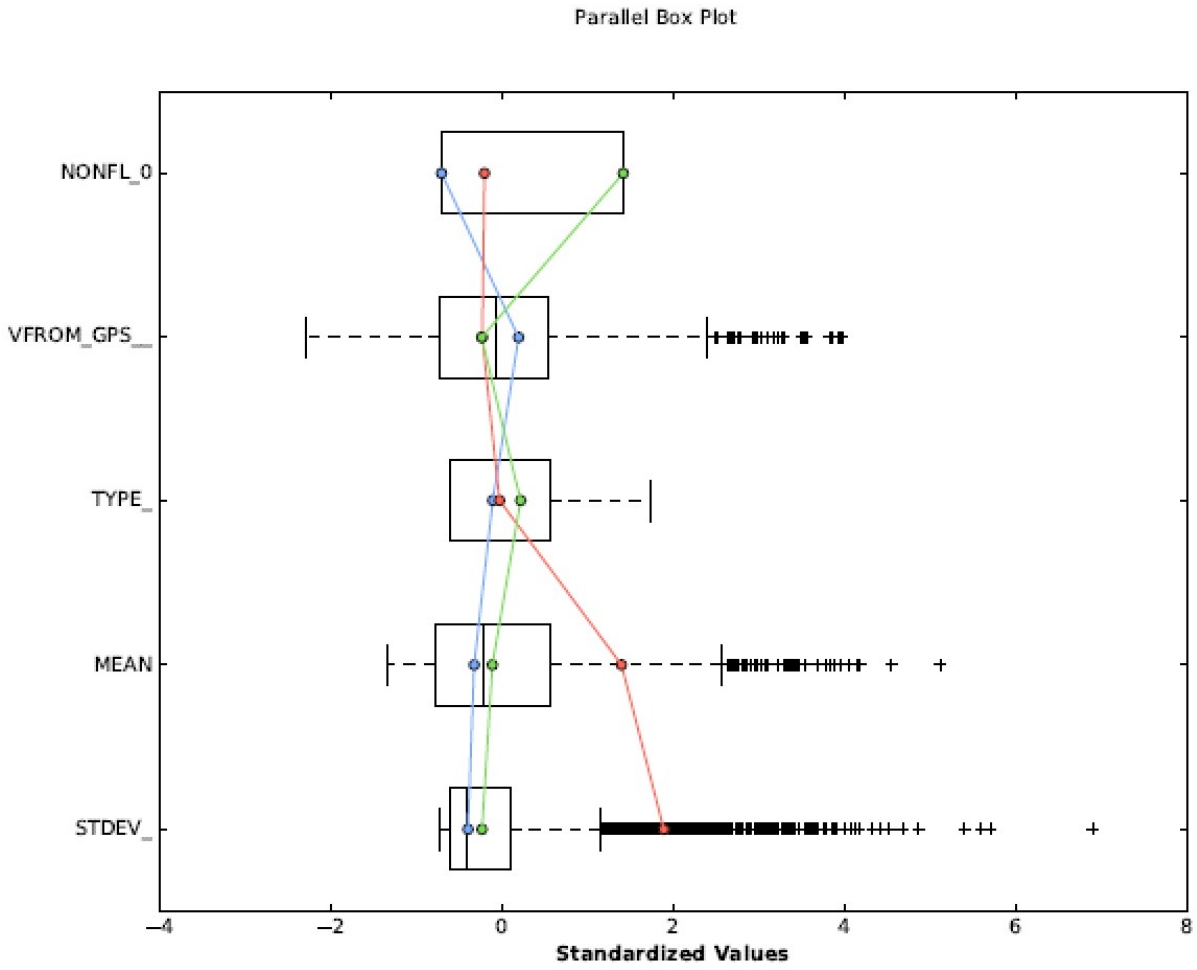

Figure 22: The parallel box plot of the 3-group analysis from Figure 20

The blue line in this plot represents group 1 in Figure 20, which are also shown in blue dots in the Figure. All points of this group are outside of the flood zone as the attribute NonFl_0 shows the 0 score for its group. This group has a higher elevation compared to the other two as can be seen from the VFROM_GPS attribute. This group contains all three of the pavement types since the TYPE score is near average. This group has the lowest Mean and Standard deviation of IRI score.

The green line in Figure 22 represents group 3 in Figure 20. The NonFl_0 attribute shows that this group belongs to points that are inside the flood zone. The elevation in this group is lower compared to group 1. Similar to group 3, this group contains all types of pavement structure, but its tendency towards higher values compared to other two groups shows that group 3 has less asphalt pavement type. Compared to group 1 which belongs to non-flooded points, this group has a slight increase in Mean and Standard deviation in IRI score from 2015 to 2019.

The red line in Figure 22 represents group 2 in Figure 20. This group contains data points that some of them are inside the flood area and some of them are outside. The average elevation is similar to one of group 3 and is lower than one of group 1. This group also contains all types of

pavement structures. The Mean and Standard deviation values of this group is significantly higher than ones of groups 1 and 3.

By adding other attributes or reducing the current ones, and also changing the number of groups, the PIs conducted a new grouping analysis based on IRI scores in the Lafayette parish with their grouping map and parallel plot box as shown in the following Figures.

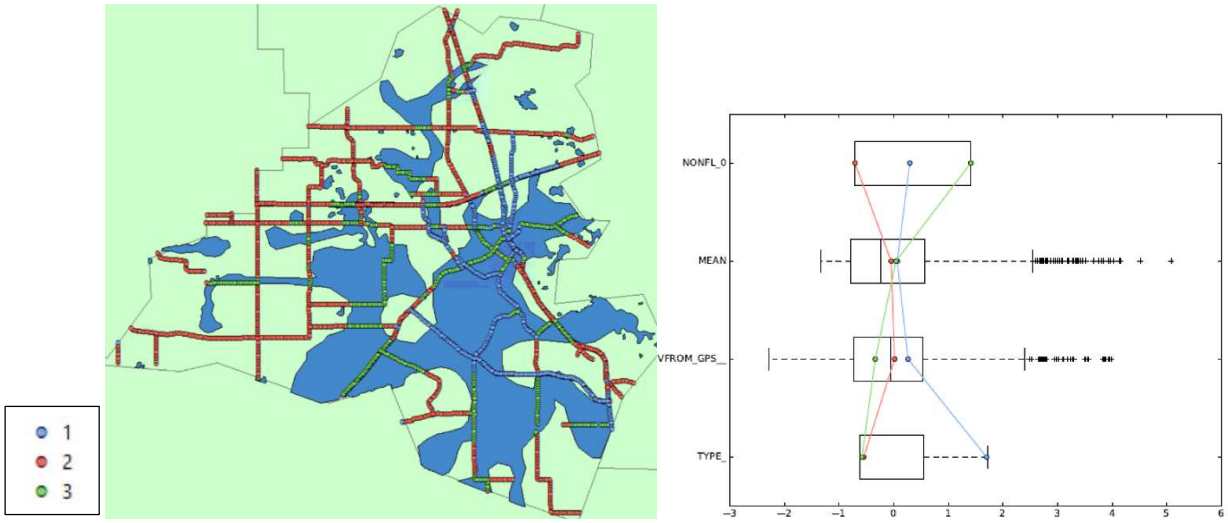

Figure 23: New grouping analysis without including standard deviation in the analysis

The IRI mean values from 2015 to 2019 are approximately the same in this grouping. Similar to the previous analysis, the elevation of points that are inside the flood zone (group 3 / green line) are lower than ones of the other groups.

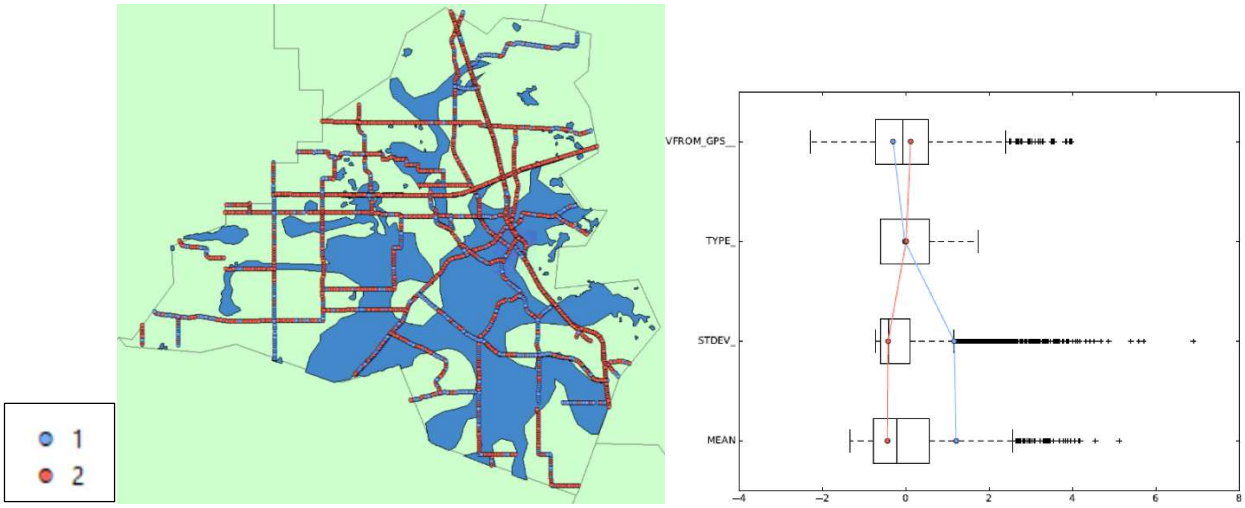

Figure 24: Grouping analysis based on two groups

The NonFl_0 is omitted from the attributes to check if the new grouping can be complied with the flood zone in the ArcMap (picture in the left). No specific pattern was not found for compliance of this clustering with the flood zone in the parish.

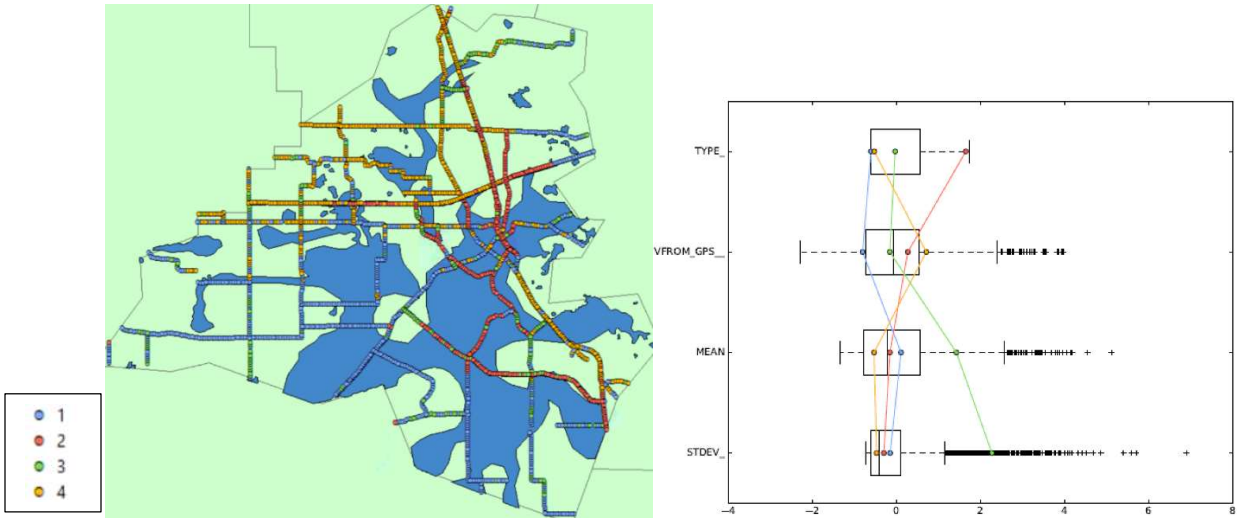

Figure 25: Grouping analysis based on four groups and without NonFl_0 attribute

This analysis was based on four groups by excluding the attribute related to flood zone (NonFl_0). This attribute is omitted to investigate the variations in other attributes and see if any relation (compliance) can be found among other attributes and flood zones. From the right-hand side of Figure 25 (the parallel box plot) it can be seen that the blue line which belongs to group 1 only clusters the asphalt pavements, which have the lowest elevation. This group has a higher mean and standard deviation compared to ones of groups 2 and 4. From the left-hand side of Figure, it is evident that the blue dots are inside the flood zone. The red line represents group 2 which it can be concluded from the type attribute in the box plot that it only contains JCP (Joint Concrete Pavements). The yellow lines represent asphalt pavement types which have the highest elevation. This group (group 3) have the lowest mean and standard deviation in IRI score. It can be seen from the map that these points are outside of the flood zone.

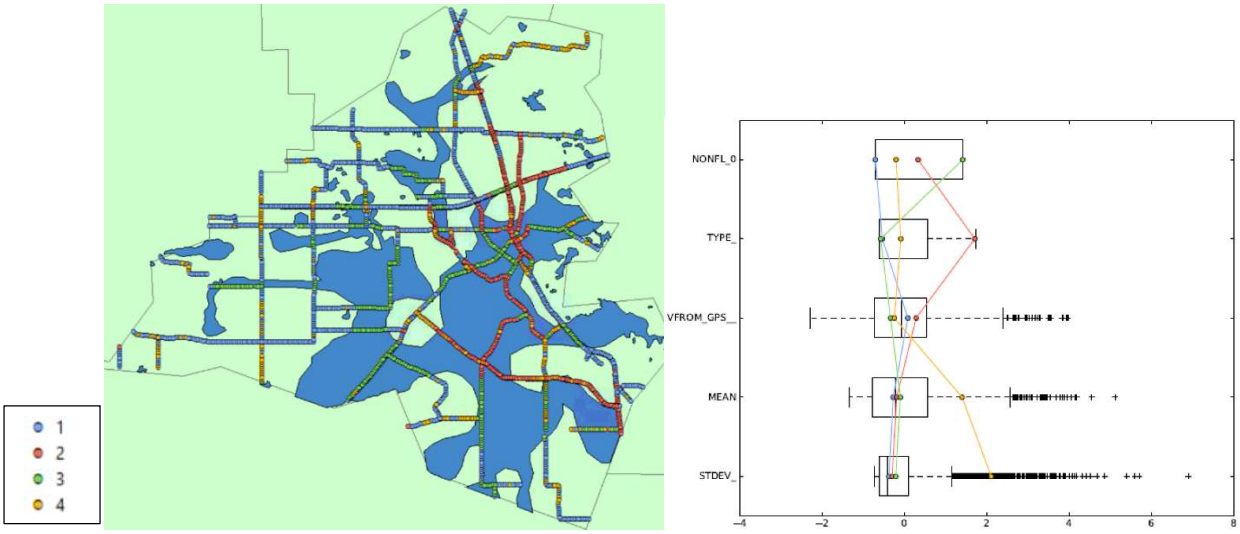

Figure 26: Grouping analysis based on four groups and with including NonFl_0 attribute

Figure 26 shows similar analysis processes with one shown in Figure 25. The difference is that in this grouping the flood zone attribute (NonFl_0) is also included. The red line that represents group 2 in the map only includes JCP pavement types that have higher average elevation compared to

ones of other groups. However, about half of the points in this group are inside the flood zone. Group 1 which are shown in blue color are the points with mostly asphalt pavements that are inside the flood area. No significant difference is evident in mean or standard deviations in IRI score for this group.

5.5. Short-term and long-term analysis

Unlike the analysis in section 3.1, which was based on mean values of the control sections, this analysis is conducted based on the values of each datapoint. The two assumptions for the increase/decrease of distress data in the previous analysis is also considered in this one. As mentioned in the description of equation 5, there are possibilities to have repairs or maintenance activities done in some control sections, and the distress data in PMS database can reduce over each consecutive year. As a result, in this analysis, the datapoints with considerable decrease in distress data (more than 10% decrease in the following year) were assumed as repaired roads and were excluded from the calculations.

Similar to the section 3.1 analysis, this analysis process is also separated into short-term and long-term, but the difference is that the calculations are conducted on every single datapoints instead of calculating the mean values of all datapoints. Another difference with the previous one is the selected control sections. In this analysis, the flooded control sections are the ones that are inside the flood zone, while in the previous analysis, the flooded control sections were the ones that were reported as flooded in the DOT report in August 2016. For each datapoint we have equation 6.

$$S_i(X) = \frac{X_{2016} - X_{2015}}{X_{2015}} \tag{6}$$

Where, S_i is the growth rate of distress data X in short-term period for each datapoint (i), X represents all types of distress data.

For calculating the long-term effect, the highest distress score during the years 2017 to 2019 were selected for each datapoint to compare with 2015 score (equation 7).

$$L_i(X) = \frac{Max(X_j) - X_{2015}}{X_{2015}}, \quad 2017 < j < 2019 \tag{7}$$

Where, L_i is the growth rate of distress scores in long-term period for each datapoint (i).

The overall growth of the distress data according to short-term and long-term periods are calculated using S_i and L_i functions in equations 6 and 7. Equations 8 and 9 are the mean values of all of the S_i and L_i of all datapoints for each distress type.

$$S_t = \frac{\sum_{i=1}^{n} S_i}{n} \tag{8}$$

$$L_t = \frac{\sum_{i=1}^{n} L_i}{n} \tag{9}$$

Where S_t is the overall growth rate of the pavement's distress in short-term, and L_t is the overall growth rate of distress in long-term period. Besides the overall analysis that include all types of pavements, this section includes analysis one each pavement type separately. In addition, traffic

data was included in the analysis to investigate the effect of traffic on flooded and non-flooded roads.

The traffic data was divided into the three categories, Low, Medium, and High according to the following range of average daily traffic (ADT):

- Low traffic volume: ADT < 10,000
- Medium traffic volume: 10,000 < ADT < 50,000
- High traffic volume: 50,000 < ADT

For each category, the short-term (ST) and long-term (LT) effect analyses were conducted separately, and the results are shown in the following tables. The empty cells in these tables indicate no data available, and the number of datapoints available for the analysis are shown in the "No." column.

Table 4: Short-term and long-term distress analysis for Low traffic pavements

Analyzed feature(s)	Flood	No.	Non-flood	No.	Flood	No.	Non-flood	No.	Comment
IRI	+19%	825	+15%	744	+19%	4,378	+21%	8,147	IRI increased in short-term for flood zones
Faulting	+33%	48	+47%	58	+32%	1,117	+35%	1,533	
PerfIndx	-3%	825	-4%	731	-12%	4,753	-11%	8,870	
Random Cr	+4%	825	+5%	727	+12%	2,956	+9%	6,037	Random cracking increased in long-term for flood areas
Roughness	+1%	849	+2%	768	+7%	4,558	+11%	8,516	Roughness increased in flood areas in long-term effect
Rutting	-4%	668	-3%	637	+0%	3,634	+1%	7,168	

Table 5: Short-term and long-term distress analysis for Medium traffic pavements

Analyzed feature(s)	Flood (ST)	No.	Non-flood (ST)	No.	Flood (LT)	No.	Non-flood (LT)	No.	Comment
IRI	+5%	1,898	+10%	2,753	+31%	1,974	+36%	2,783	
Faulting	+52%	355	+39%	540	+39%	380	+40%	665	Faulting increased in both short-term and long-term effect in flood zones
PerfIndx	-3%	1,851	-3%	2,756	-13%	2,313	-14%	3,286	
Random Cr	+3%	1,270	+3%	1,941	+4%	782	+6%	1,282	
Roughness	+1%	2,095	+1%	3,024	+3%	1,861	+7%	2,670	Roughness slightly increased in long-term for flood areas
Rutting	-2%	1,102	-3%	1,737	-0%	1,192	+2%	1,955	Rutting slightly increased in long-term for flood areas

Table 6: Short-term and long-term distress analysis for High traffic pavements

Features	Flood (ST)	No.	Non-flood (ST)	No.	Flood (LT)	No.	Non-flood (LT)	No.	Comment
IRI	+6%	334	+7%	1,224	+18%	355	+16%	1,133	
Faulting	+54%	60	+49%	138	+40%	57	+45%	185	Faulting increased in both short-term and long-term analysis
PerfIndx	-2%	347	-3%	1,230	-8%	377	-8%	1,321	
Random Cr	+4%	85	+3%	390	+1%	57	+1%	228	Random cracking slightly increase for long-term effect
Roughness	+1%	365	+0%	1,336	+1%	326	+3%	1,258	
Rutting	-2%	79	-3%	282	-3%	71	-2%	315	

5.6. Analysis results and comparison

Estimated 2016 flood maps show the affected areas in 2016 Louisiana flood. The left-hand side of Figure 27 shows the flood prone areas according to the FEMA flood maps, and the right side illustrates the estimated flooded areas in the 2016 Louisiana flood obtained from the ArcGIS online maps.

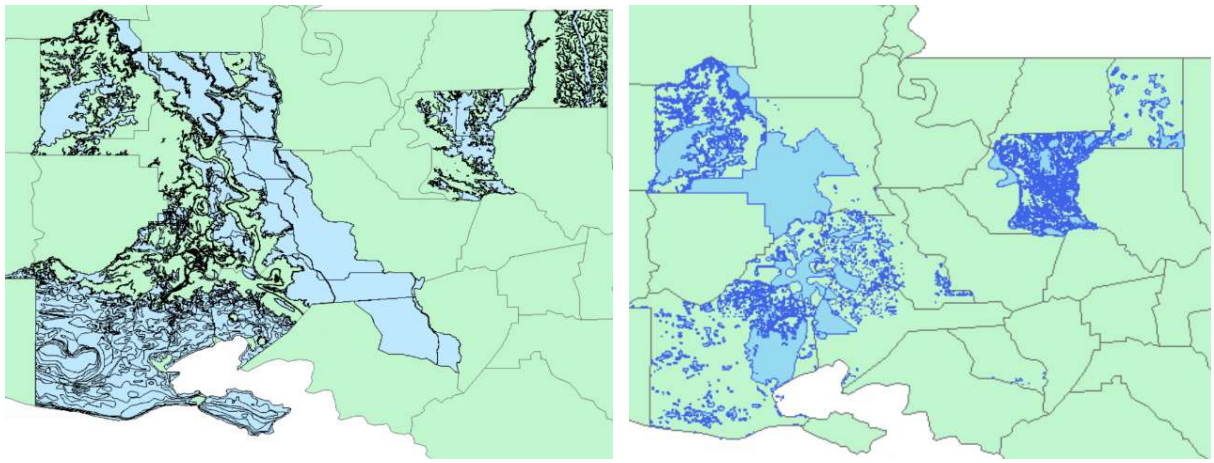

Figure 27: Studied parishes with highlighting the high-risk flood zones (Left: FEMA flood maps. Right: Estimated flood areas in 2016 Louisiana flood from ArcGIS online maps)

As these two maps cover different areas shown in Figure 27, the PIs analyzed only the areas with high risk of flood (A, AE, and AV) in the FEMA flood zone map. In the analysis according to FEMA flood areas, the PMS data points inside the high-risk flood zones were detected and distinguished from the points outside of the flood area. The total number of data points that were involved in this study was 26,330, with 7,512 inside the high-risk flood area and 18,817 outside.

In the analysis according to estimated flood 2016 flood, the PMS data points inside the flood zones were detected and distinguished from the points outside of the estimated flood area. The total number of data points that were involved in this study was 26,330, with 9,393 inside the high-risk flood area and 16,936 outside.

Figure 28 bellow shows the overall analysis of comparing the distress scores between the data points inside and outside high-risk flood area. The left-hand side are the results of the analysis based on FEMA and the right-hand side are the results of the analysis according to estimated 2016 flood maps.

The comparison shows significant changes between the flood and the non-flood distress scores when using estimated flood maps compared to ones using FEMA flood maps. IRI increased slightly in the flood areas. No significant difference can be seen in the Faulting scores in both the flood and the non-flood analyses and the performance index dropped in the flooded areas.

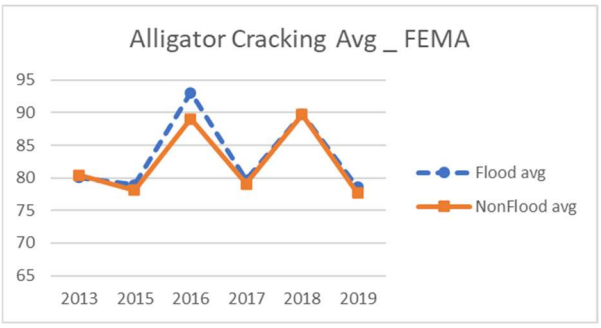

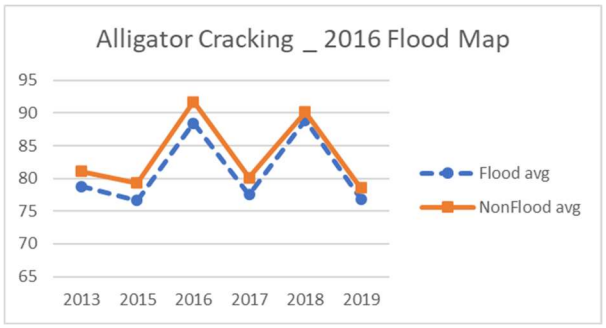

FEMA flood zone ArcGIS estimated 2016 flood

Alligator cracking

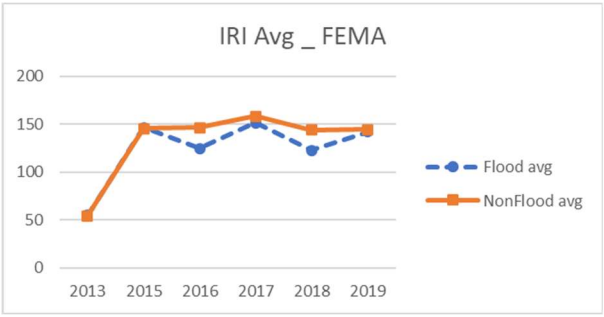

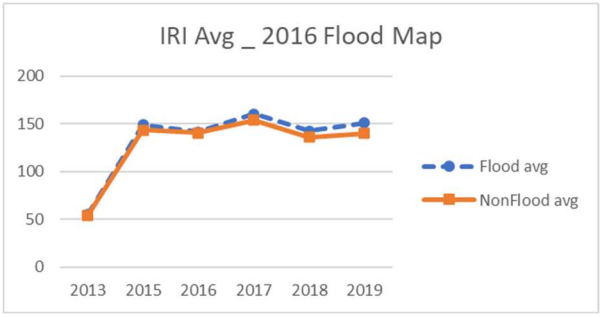

FEMA flood zone ArcGIS estimated 2016 flood

IRI

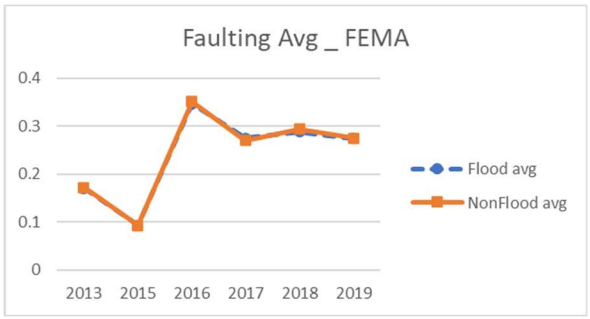

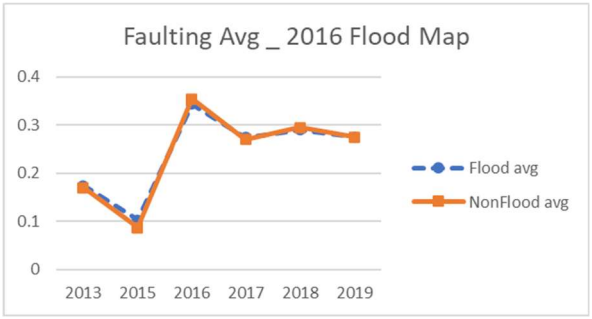

FEMA flood zone ArcGIS estimated 2016 flood

Faulting

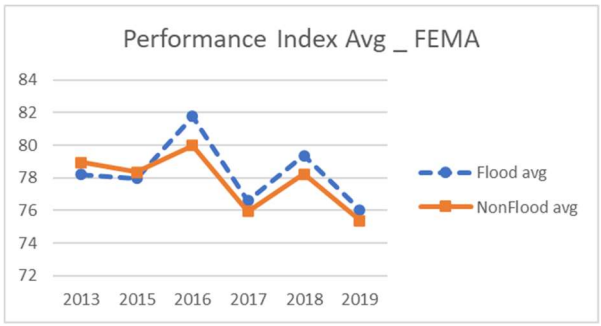

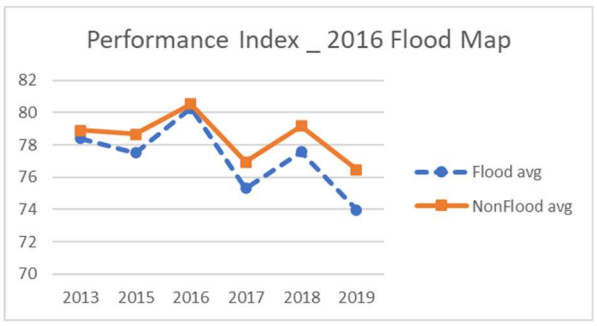

FEMA flood zone ArcGIS estimated 2016 flood

Performance index

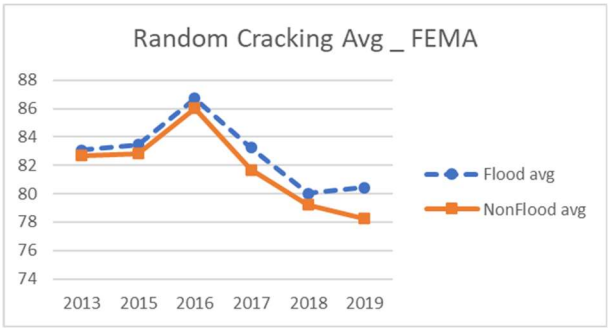

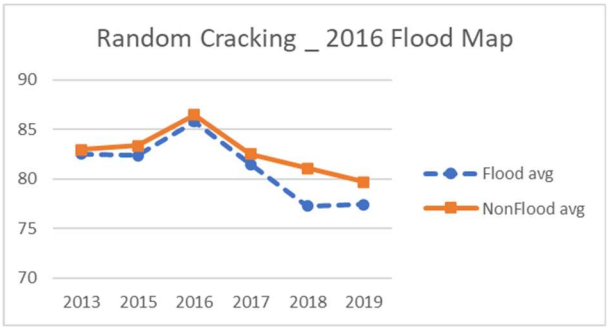

FEMA flood zone ArcGIS estimated 2016 flood

Random cracking

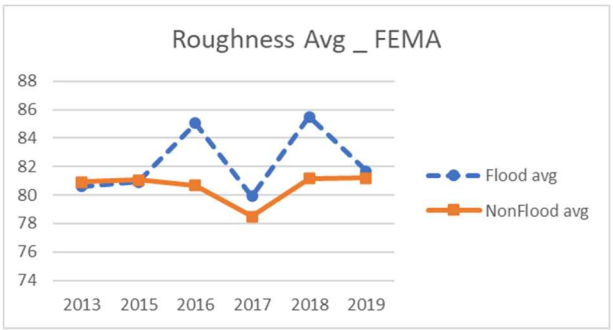

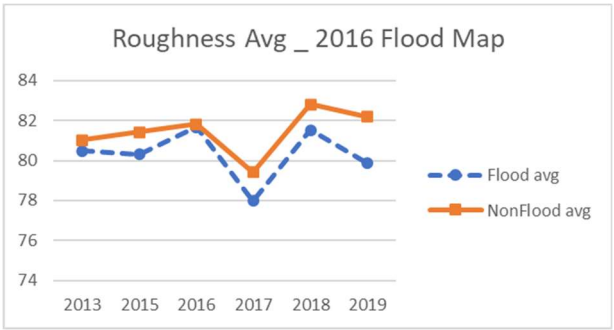

FEMA flood zone ArcGIS estimated 2016 flood

Roughness

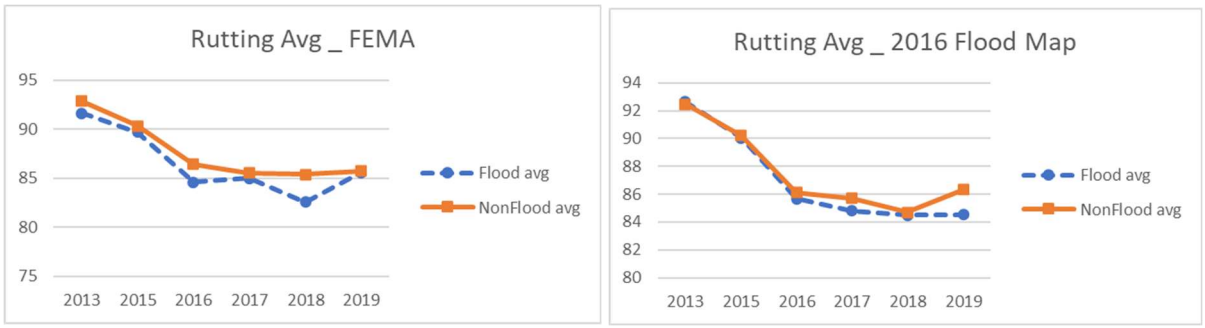

FEMA flood zone ArcGIS estimated 2016 flood

Rutting

Figure 28: Average distress scores for flood areas and non-flood areas and a comparison between the analysis according to FEMA flood maps and ArcGIS estimated 2016 Louisiana flood

5.7. Prediction model

According to Reza et al. (2005), performance of a pavement is a comprehensive assessment of a pavement condition that involves characterization of skid resistance, structural adequacy, roughness, and surface distress (Reza et al. 2005). The performance index attained from the Louisiana PMS data was analyzed in the previous sections. The score is between 0 and 100, and according to the analysis in section 3.5, which is based on estimated 2016 flood maps, the performance index is affected by flood. Reza et al. categorized the performance index into the following five groups as shown in Figure 29.

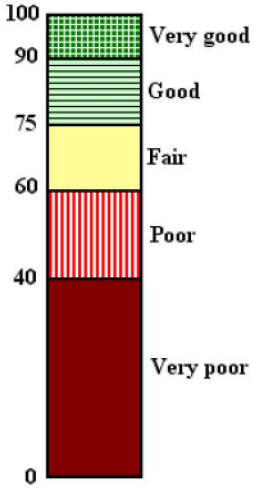

Figure 29: Categorization of pavement performance index by (Reza et al. 2005)

According to this categorization, the performance index scores between 0 and 40 were considered as very poor in this categorization. Scores between 40 and 60 were considered as poor, 60 to 70 as fair, 75 to 90 as good, and the scores above 90 were considered as very good.

5.7.1. Prediction model based 2016 flood data

Various datasets were created on the PMS data, and two different prediction models were applied on each dataset to find the prediction model and the dataset with highest accuracy. The chosen dataset has the following characteristics.

Dataset attributes:

- Repair and rehabilitation data
- Average faulting 2013
- Average faulting 2015
- Random cracking 2013
- Random cracking 2015
- Roughness 2013
- Roughness 2015
- Rutting 2013
- Rutting 2015
- Number of patching and potholes 2013
- Number of patching and potholes 2015
- Average IRI 2013
- Average IRI 2015
- Performance index 2013
- Performance index 2015
- Flood data (based on estimated 2016 flood in Louisiana)
- Traffic data
- Pavement type

Target value:

- Performance index 2017

The label of the dataset was the performance index of the pavement in 2017, the year after the 2016 flood event in Louisiana. 80% of the data were selected for training and the remaining 20% were selected for testing. The most accurate prediction model for this dataset was the XG Boost (XGB) classifier with the following confusion matrix. XG Boost is a decision-tree-based highly efficient optimized library that uses ensemble technique for implementing a machine learning algorithm on the datasets. The target variable in this study is the pavement performance index in the year 2017, and the model initializes with the function F0(x) which minimizes the loss function (mean squared error) using the following formula;

$$F0(x) = argmin \sum_{i=1}^{n} (y_i - \gamma)^2 \quad (10)$$

Gamma (γ) is the similarity measure between the prediction and target value. The boosting model could be initiated with the following formula since with respect to γ, the function initializes at the mean, i =1 (29).

$$F_0(x) = \frac{\sum_{i=1}^{n} y_i}{n} \quad (11)$$

The predictions are provided by the above function and the new residual for each record will be (yi – F0(x)). This process continues until it reaches to the optimum value which is the maximum reduction of errors. The diameter of the matrix shows the number of correct predictions in the test set.

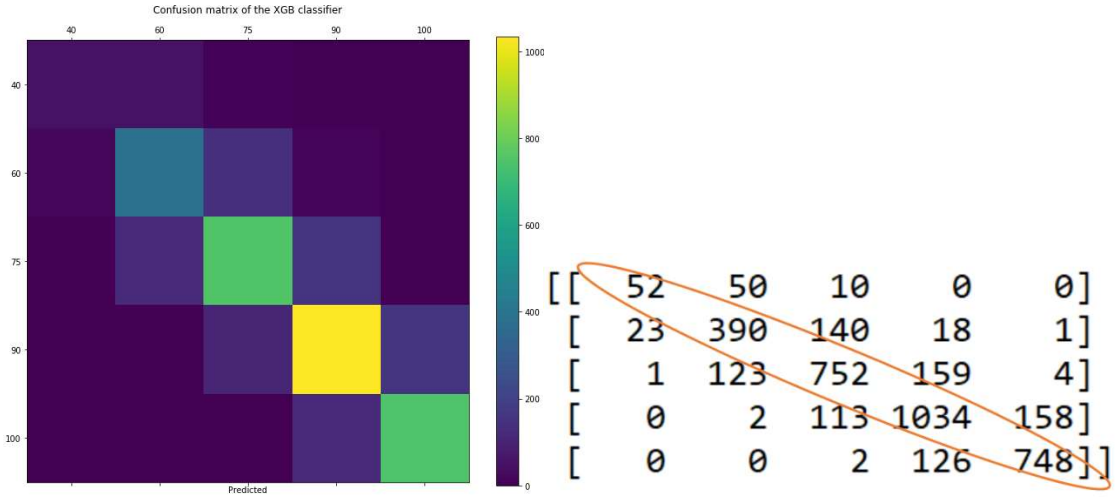

Figure 30: Confusion matrix of the XGB prediction model

The accuracy of the above model is 76.19 percent.

Support vector machine (SVM) was also used for this dataset, but the accuracy is 70.12 percent, which is slightly lower than one of XGB. The confusion matrix for SVM is shown in the following figure.

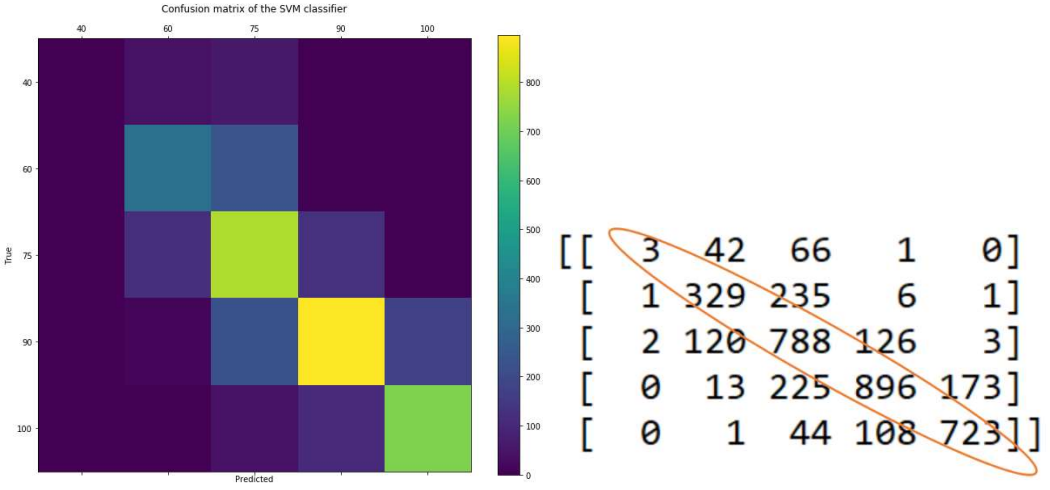

Figure 31: Confusion matrix of the SVM prediction model

5.7.2. Prediction model based on FEMA flood maps

To create a prediction model for pavement performance, the PIs used FEMA flood maps that can help distinguish the data points inside the flood zone from the data points outside the flood zone.

A dataset with the same attributes of repair data, distress data, traffic data, and pavement type, was created, but the FEMA flood data used in this study was different from ones used in the previous analysis. The XGB prediction algorithm was applied to the new dataset, and results are shown in Figure 32.

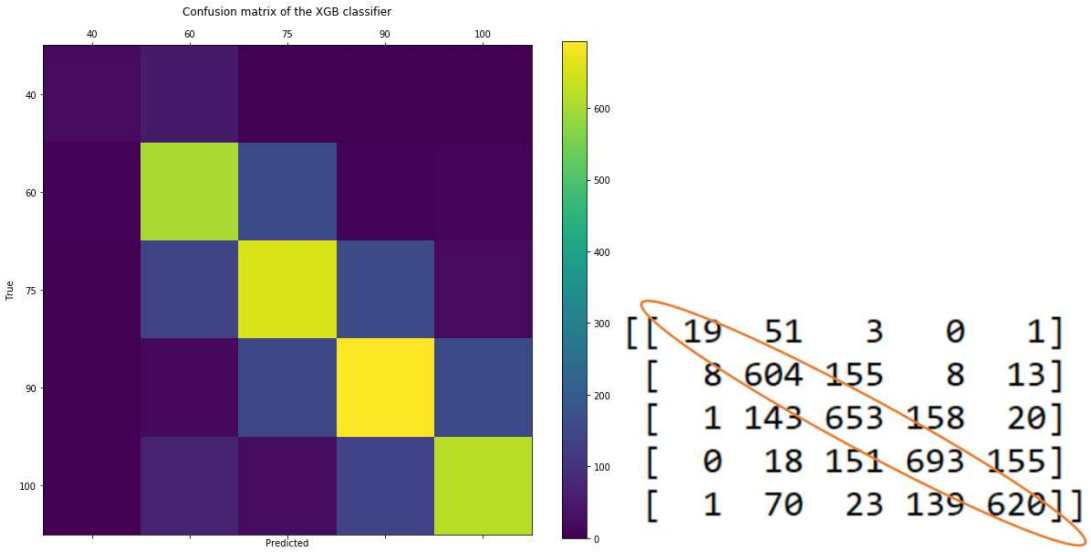

Figure 32: Confusion matrix of the XGB prediction model for the dataset with FEMA flood data

The accuracy of the above prediction model is 69.8 percent. This result shows that the dataset with the 2016 flood data is about 7 percent more accurate than one of the prediction model on the dataset with the FEMA flood data. Thus, it can be concluded that, the 2016 flood data is more compatible with the pavement performance scores. In other words, the 2016 flood data more accurately shows the effect of flood on pavement performance and is a proper source for a prediction model.

For an overall prediction of pavement performance, the accuracy of the prediction model with the dataset with the FEMA flood data can be enhanced by increasing the number of attributes. The previous prediction models predict the 2017 pavement performance. To predict the pavement performance of 2019, it is needed to add the 2017 data to the dataset. To illustrate, a new dataset was created with the following attributes, and target value.

Two prediction models were used for the PMS dataset with the FEMA flood data. The chosen dataset has the following characteristics. The attributes for each record of the dataset are as follows:

Dataset attributes:

- Repair and rehabilitation data
- Random cracking 2013
- Random cracking 2015
- Random cracking 2017

- Roughness 2013
- Roughness 2015
- Roughness 2017
- Rutting 2013
- Rutting 2015
- Rutting 2017
- Number of patching 2013
- Number of patching 2015
- Number of patching 2017
- Average IRI 2013
- Average IRI 2015
- Average IRI 2017
- Performance index 2013
- Performance index 2015
- Performance index 2017
- Flood data (based on FEMA flood maps)
- Traffic data
- Pavement type

Target value:

- Performance index 2019

The label of the data set was the performance index of the pavement in 2019.

The most accurate prediction model for this dataset was the XGB classifier with the following confusion matrix.

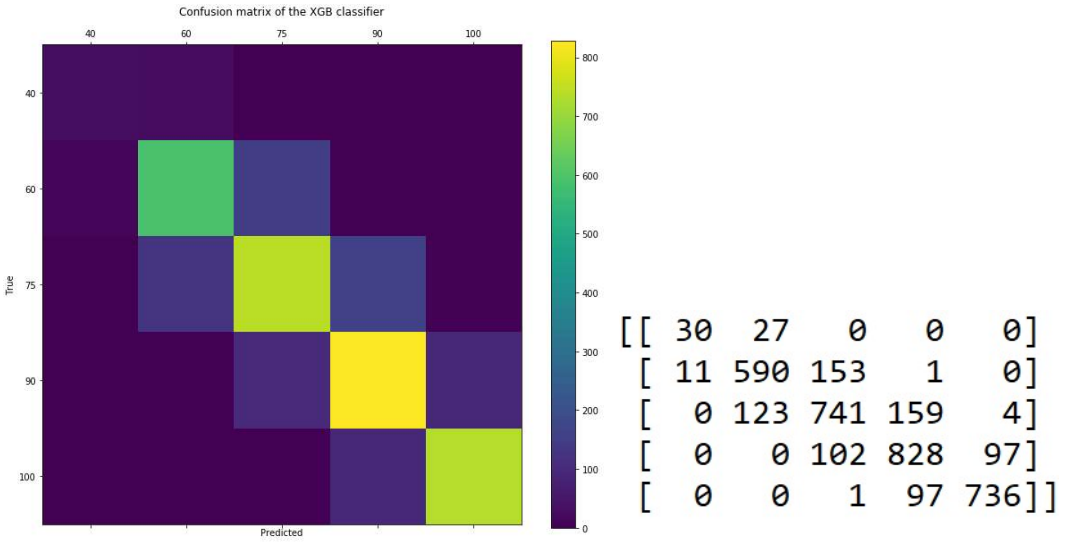

Figure 33: Confusion matrix of XGB classifier applied on the dataset with FEMA flood data and 2013 to 2017 PMS data for predicting pavement performance in 2019

The accuracy of the above model is 79.05 percent.

Support vector machine was also used for this dataset, but the accuracy is 71 percent, which is slightly lower than one using XGB. The confusion matrix for SVM is shown in the following figure.

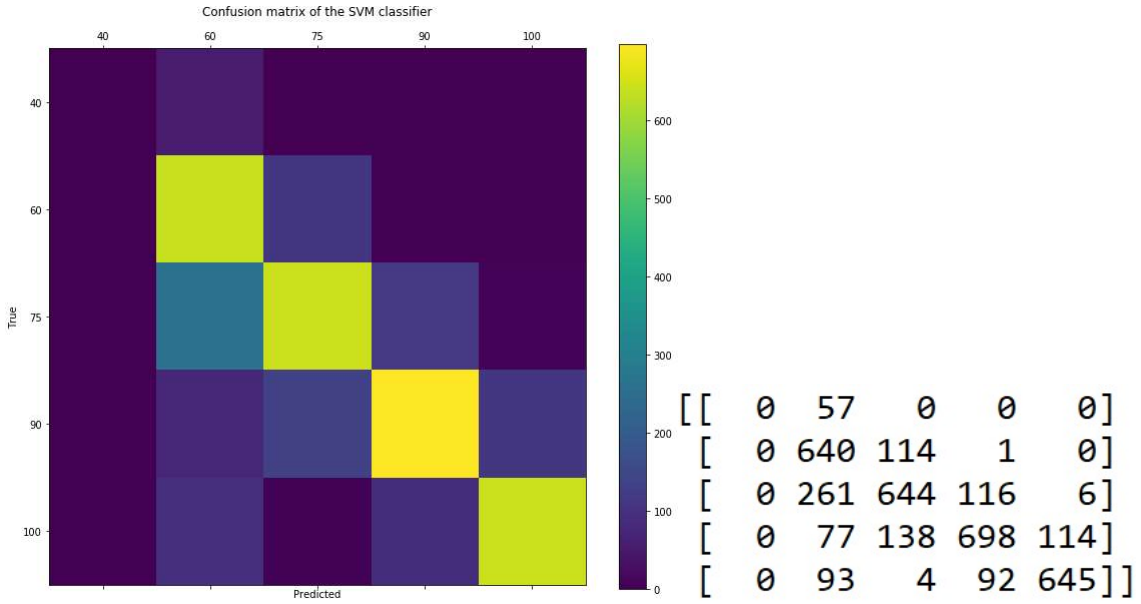

Figure 34: Confusion matrix of SVM classifier applied on the dataset with FEMA flood data

The accuracy of these two models (that was based on the FEMA flood maps) were higher than ones of the prediction models based on estimated 2016 flood maps. The reason of this increase in accuracy was that this analysis contains larger number of historical data in FEMA datasets. The dataset with 2016 flood data, the 2013 and 2015 PMS data were used to predict the pavement performance in 2017. Whereas in the FEMA dataset the PMS data of 2013, 2015, and 2017 were used to predict the pavement performance in 2019. Increasing the number of records also increased the accuracy regardless which dataset we use.

5.7.3. Testing and implementation of the prediction model

Among 26,330 records contained in the dataset, 1,000 records were excluded to create a new dataset for testing the developed prediction model and evaluate the accuracy of the predicted data with the real data. Figure 35 shows the entire 1000 datapoints in the map.

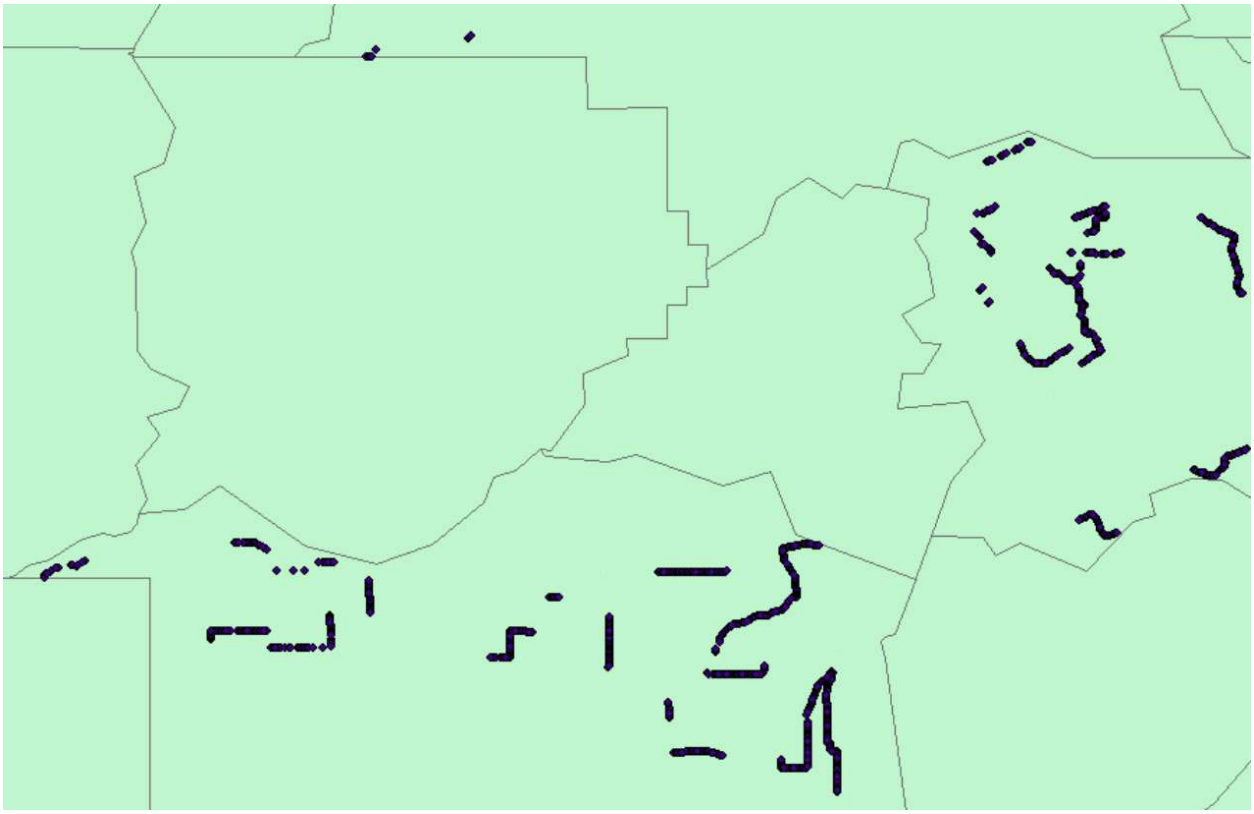

Figure 35: The 1000 data points that were excluded from the dataset for testing the model

The prediction model was applied to the new test set with the historical data of 2013 and 2015 along with 2016 flood data and also the traffic data for each control section. The target value was the performance of each pavement in 2017, a year after the flood occurrence. Pavements that were predicted as poor performance were distinguished from the test set. Figure 36 shows the datapoints that were predicted to have a poor performance in 2017.

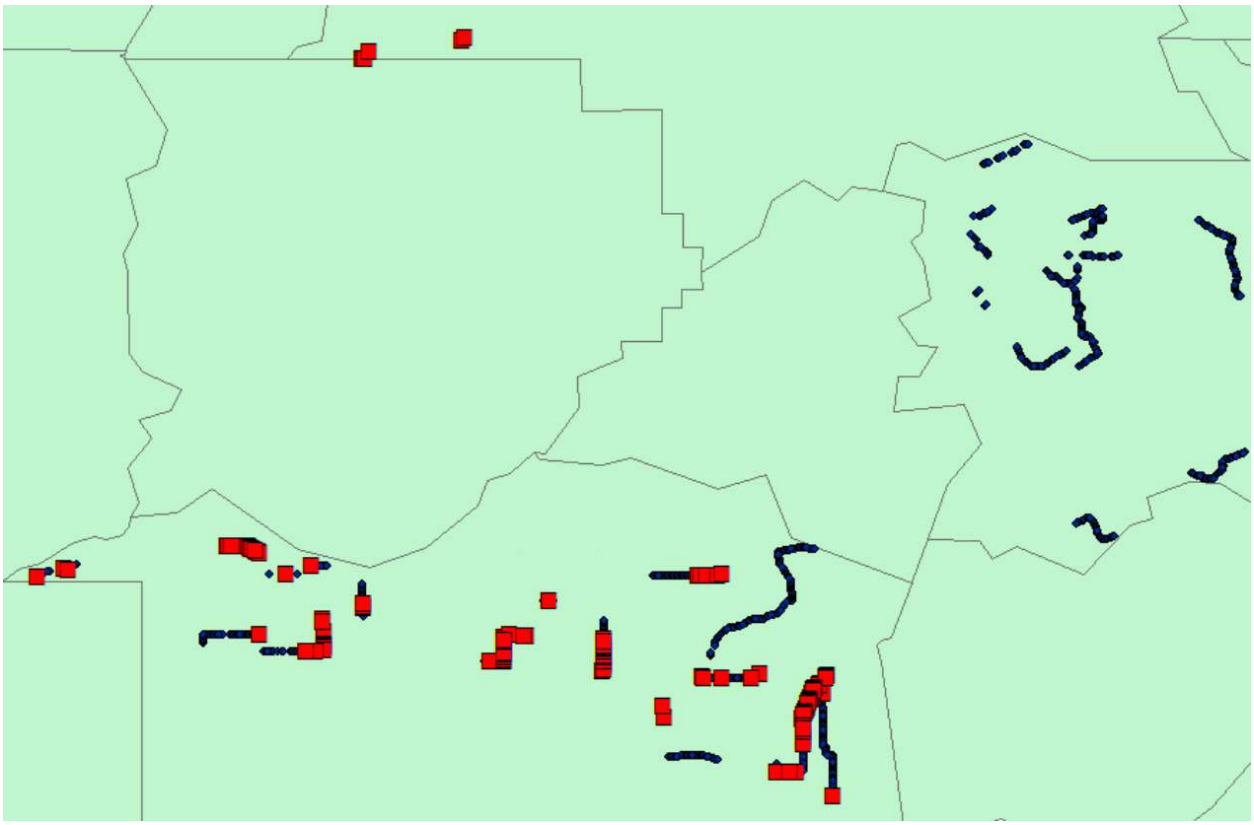

Figure 36: The poor performance predicted pavements in red square

The pavements with poor performance (see Figure 29 for performance categorization) are distinguished with the red squares. At this stage we need to comply the predicted datapoints with real datapoints that had poor performance in 2017 (Figure 37).

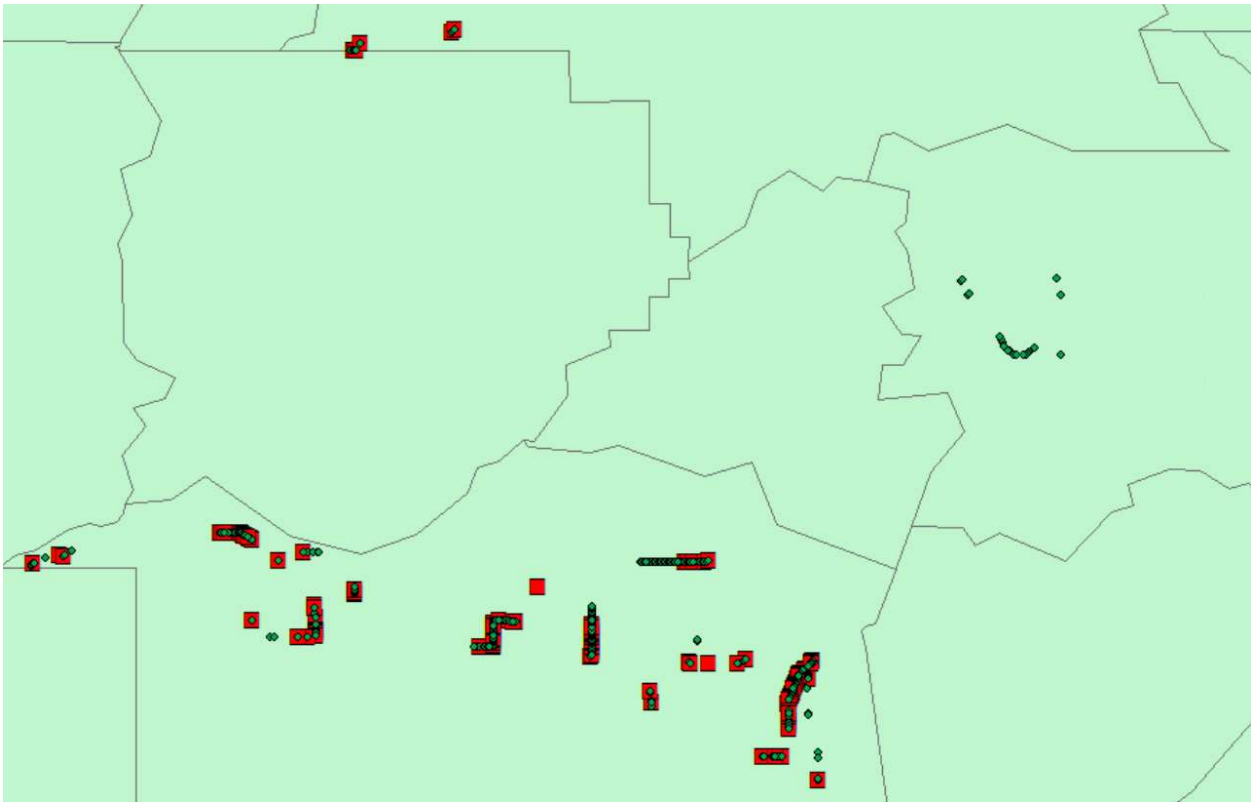

Figure 37: Comparing the prediction (red squares) with the real data (green dots)

The predictions of pavements with poor performance in 2017 shown in the red squares and the green dots illustrate the real poor pavements in 2017. As shown in Figure 37, the prediction mostly complies with the real data, although there are data points that the model cannot accurately predict. To rectify this inaccurate prediction and enhance the model's accuracy, the method is needed to include the large number of records.

6. CONCLUSIONS

The primary objective of this research study is to create a network level analysis of pavement performance during and after flood events using the pavement condition data and historical flooding maps. To this end, PMS data accumulated over 10 years in Louisiana and pavement condition data collected in the city of Houston were utilized, and diverse analyses were conducted accordingly to figure out meaningful relationships among several features, pavement characteristics, and possible factors such as pavement performance indicators, pavement's location, elevation, and others. In summary, this study provided the following four different types of analyses on the pavement condition data:

(1) Simple analyses by identifying the flooded roadways in both Louisiana and Texas, and comparing the pavement performance before and after the flood event.
   - Using DOTD reports for detecting the flooded roads and control sections in the East Baton Rouge Louisiana.
   - Using ArcMap Online maps to identify the flooded roadways in Houston Texas.

(2) Analyses based on FEMA flood zones, which used the flood zone maps to distinguish between the control sections that are inside the flood zone and those that are outside.

(3) Clustering analyses that can be divided into the two different analyses.
   - Single feature cluster analyses, which investigated the statistical characters of a single attribute such as IRI and comply them with flood zone feature map.
   - Multiple feature cluster analyses (grouping analysis), which conducted analysis based on several features to find clusters of datapoints with similar statistical characters based on various attributes.

(4) Short-term and long-term analyses.

The first analysis showed that there can be inconsistencies in the pavement condition data. With clearly identified flooded and non-flooded areas in the city of Houston, the comparison analyses of the pavement performance of roadways were conducted with different categorization: traffic levels, pavement types, and roadway types. For instance, the average IRI score during the consecutive years are decreased for some of the control sections, while it is expected to see an increase in the IRI as time passes. These abnormal data were found in Louisiana PMS data and the city of Houston data. This can be the result of road maintenance or rehabilitation for those control sections or can be errors. In particular, even though the city of Houston data shows performance deterioration after the 2017 Hurricane Harvey event, because of these unknown variables, the PIs were not able to confidently conclude the level of flood impacts on pavement. Although the clustering analyses showed interesting clusters of data points in some areas, it is still challenging to infer any hypotheses, and require additional in-depth analyses with expert opinions.

The results of the analyses based on the FEMA flood maps, compared to the analyses according to the 2016 estimated Louisiana flood maps, were considerably heterogeneous. The IRI scores in the flooded areas were lower in flood areas based on the FEMA map, whereas they were slightly higher based on the 2016 estimated flood data. Performance index were considerably lower in flood areas according to the 2016 flood maps, while they were higher according to the FEMA map.

One of primary outcomes in this study is the prediction model, which showed that the scores range of pavement performance is predictable with 76% accuracy using historical data such as previous distress data, traffic data, flood data, and others. The control sections of eight parishes involved in this study provided a total number of 26,330 records for the dataset required for prediction. Prediction can be improved by involving more datapoints form the remaining parishes, but this requires data such as flood inundated roads which for the 2016 flood event, are not available for every parish.

In this research study, the PIs had a limited access to the pavement condition data of Texas because the Texas Department of Transportation (TxDOT) considers the pavement condition data as sensitive information and maintains a strict policy to keep their pavement data confidential. Thus, the PIs communicated with the city of Houston and obtained the limited dataset of the PCI scores collected from 2016 to 2018, which were utilized in this study. Since this dataset uses the PCI scores to measure the pavement conditions not including the detailed distress types and their values, the PIs employed the detailed and long-term PMS data provided from LA DOTD to conduct clustering analyses and develop a consistent and robust prediction method.

The PIs believe that this flooding before-and-after analysis is expected to be a critical benchmark that helps reduce the cost of obtaining structural composition data for a direct damage analysis such as less number of cores/bores. Furthermore, this new method facilitates integrated pavement maintenance based on revealed network-level patterns of pavement flood damage. The information of pavement damage caused by flooding disasters is also crucial for Region 6's States for the preparation of the claims (quantities) made to FEMA Federal Emergency if they encounter a flooding disaster in the future. In addition, the predictive models can help determine the reliable post-flood maintenance costs of flexible type pavement reconstruction projects. With diverse perspectives to evaluate the PMS data, this project established the first view and systematic post-flood analysis that practitioners in DOTs can use to prioritize and predict pavement management issues and rehabilitation practices. Moreover, this project helps make a well-guided decision on the integrated pavement damage recovery and facilitate a synergetic effort to leveraging the uses of the current PMS and Pavement Analytics systems of Louisiana and Texas.

This study addresses urgent Texas and national challenges by providing immediately applicable solutions for the resilient roadway renewals of post-disaster damages. This project will provide LaDOTD and TxDOT with a guidebook that clearly describes systematic procedures for identifying regional pavement damage patterns on the flood model. The research outcomes are therefore expected to bring new scientific knowledge on the implications of post-flood damages on transportation infrastructure. In addition, the intellectual merit of this research study includes a holistic investigation into a network-level PMS/Pavement Analytics data analysis approach (in which parameters and feasible regions vary in time) for unveiling latent post-flood pavement damage patterns. Furthermore, a prediction model of post-flood pavement performance will be new formalized scientific knowledge that will be helpful for practitioners and following researchers. The investigation of post-flood pavement damage evaluation helps practitioners and communities better understand the impact and economic factors (barriers and enablers) of flood disaster on transportation infrastructure.

REFERENCES

1. Pielke RA, Gratz J, Landsea CW, Collins D, Saunders MA, Musulin R. Normalized hurricane damage in the United States: 1900-2005. Nat Hazards Rev. 2008;9(1):29–42.
2. FEMA. Policies for Guiding Planning for Post-Disaster Recovery and Reconstruction. Washington D.C.; 2005.
3. Goodyear R. Housing in greater Christchurch after the earthquakes Trends in housing from the Census of Population and Dwellings 1991 – 2013. 2013. 82 p.
4. Rowley K. GulfGov Reports: The Role of Community Rebuilding Plans in the Hurricane Recovery [Internet]. Vol. 9, Nelson A. Rockefeller Institute of Government and Public Affairs Research Council of Louisiana. 2008. Available from: http://www.rockinst.org/disaster_recovery/
5. Chang SE, Nojima N. Measuring post-disaster transportation system performance: the 1995 Kobe earthquake in comparative perspective. Transp Res Part A Policy Pract [Internet]. 2001;35(6):475–94. Available from: https://ideas.repec.org/a/eee/transa/v35y2001i6p475-494.html
6. Karlaftis MG, Kepaptsoglou KL, Lambropoulos S. Fund allocation for transportation network recovery following natural disasters. J Urban Plan Dev. 2007;133(1):82–9.
7. Ferreira A, Picado-Santos L De, Wu Z, Flintsch G. Selection of pavement performance models for use in the Portuguese PMS. Int J Pavement Eng. 2011;12(1):87–97.
8. Yan H, Flores R. Louisiana flood: Worst US disaster since Hurricane Sandy, Red Cross says [Internet]. CNN. 2016 [cited 2020 Sep 3]. p. 1–4. Available from: http://www.cnn.com/2016/08/18/us/louisiana-flooding/
9. Chen X, Zhang Z. Effects of hurricanes katrina and rita flooding on louisiana pavement performance. Geotech Spec Publ. 2014;(239 GSP):212–21.
10. USGS. MAP LAYERS Real-time stream and rain gage layers only available at zoom level 9 and above. Please zoom in to view. [Internet]. 2020 [cited 2020 Mar 10]. p. 6533. Available from: https://stn.wim.usgs.gov/FEV/#LouisianaAugust2016
11. Mallick RB, Tao M, Daniel JS, Jacobs J, Veeraragavan A. Development of a methodology and a tool for the assessment of vulnerability of roadways to flood-induced damage. J Flood Risk Manag. 2017;10(3):301–13.
12. NCHRP. Quality management of pavement condition data collection. A synthesis of highway practice. Washington, D.C.; 2009.
13. Ruotoistenmäki A, Seppälä T, Kanto A. Comparison of Modeling and Measurement Accuracy of Road Condition Data. J Transp Eng. 2006;2(February 2006):482–8.
14. El-Anwar O, Ye J, Orabi W. Innovative Linear Formulation for Transportation Reconstruction Planning. J Comput Civ Eng. 2016;30(3):1–13.
15. Pradhan, Anu; Laefer, Debra F.; Rasdorf WJ (William J. Infrastructure Management Information System Framework Requirements for Disasters. J Comput Civ Eng. 2007;3801.
16. Burton CG. Social vulnerability and hurricane impact modeling. Nat Hazards Rev.

2010;11(2):58–68.

17. Watson CC, Johnson ME. Hurricane loss estimation models: Opportunities for improving the state of the art. Bull Am Meteorol Soc. 2004;85(11):1713–26.

18. Zhang Z, Wu Z, Martinez M, Gaspard K. Pavement Structures Damage Caused by Hurricane Katrina Flooding. J Geotech Geoenvironmental Eng. 2008;134(5):633–43.

19. Khan MU, Mesbah M, Ferreira L, Williams DJ. Estimating pavement's flood resilience. J Transp Eng Part B Pavements. 2017;143(3):1–8.

20. Oyediji R, Lu D, Tighe SL. Impact of flooding and inundation on concrete pavement performance. Int J Pavement Eng [Internet]. 2019;0(0):1–13. Available from: https://doi.org/10.1080/10298436.2019.1685671

21. Tighe SL. VULNERABILITIES AND DESIGN CONSIDERATIONS FOR PAVEMENT INFRASTRUCTURE IN LIGHT OF CLIMATE CHANGE. In: Conference of the Transportation Association of Canada [Internet]. Charlottetown; 2015. p. 54–67. Available from: http://repositorio.unan.edu.ni/2986/1/5624.pdf

22. AASHTO. Mechanistic Empirical Pavement Design Guide: A Manual Practice. Aashto. 2015. 218 p.

23. Lu D, Tighe SL, Xie WC. Impact of flood hazards on pavement performance. Int J Pavement Eng [Internet]. 2018;0(0):1–7. Available from: https://doi.org/10.1080/10298436.2018.1508844

24. Dawson TA. EVALUATION OF PAVEMENT MANAGEMENT DATA AND ANALYSIS OF TREATMENT EFFECTIVENESS USING MULTI-LEVEL TREATMENT TRANSITION. 2012.

25. Moravec E. Texas officials: Hurricane Harvey death toll at 82, 'mass casualties have absolutely not happened.' The Washington Post. 2017. p. 29–31.

26. Houston Community Data Connections. Hurricane Harvey. ArcGIS. 2017.

27. ArcGIS Online. Houston Flooded Roads 8-31 to 9-09. ArcGIS. 2020. p. 9–10.

28. Reza F, Boriboonsomsin K, Bazlamit SM. Development of a Composite Pavement Performance Index. (Final Rep ST/SS/05-001) Ohio Dep Transp Columbus, OH [Internet]. 2005;(January). Available from: https://www.researchgate.net/publication/311385878%0Ahttps://trid.trb.org/view.aspx?id=917555

29. Sundaram RB. Analytics Vidhya [Internet]. 2018. Available from: https://www.analyticsvidhya.com/blog/2018/09/an-end-to-end-guide-to-understand-the-math-behind-xgboost/